

AD-A143 012

ELECTRON CHARGING AND SGEMP (SYSTEM GENERATED
ELECTROMAGNETIC PULSE) STUD. (U) MISSION RESEARCH CORP
SAN DIEGO CA J D RIDDELL ET AL. 01 JAN 83 MRC/SD-R-112

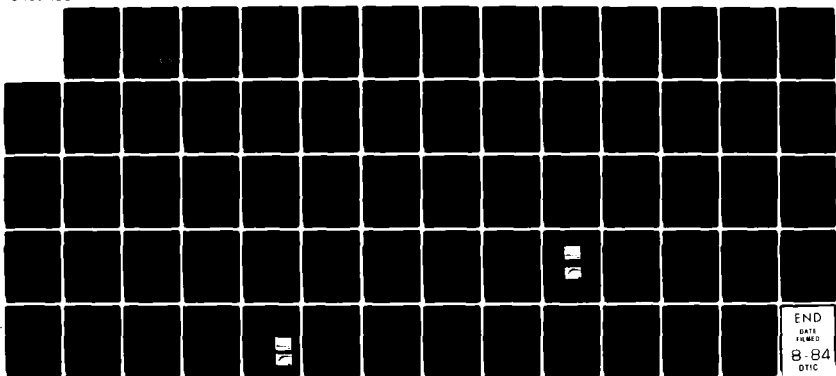
1/1

UNCLASSIFIED

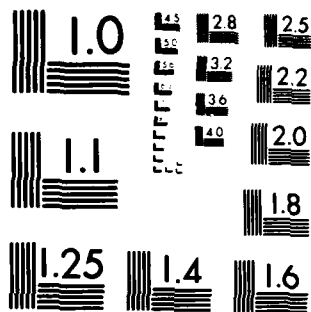
DNA-6212F DNA001-79-C-0083

F/G 22/2

NL



END
DATA
FILMED
8-84
DTIC



MICROCOPY RESOLUTION TEST CHART
NATIONAL BUREAU OF STANDARDS 1963-A

(12)

117-6 5017-1

DNA 6212F

ELECTRON CHARGING AND SGEMP STUDIES ON SATELLITE DIELECTRICS

AD-A143 012

J. D. Riddell V. A. J. van Lint
B. C. Passenheim D. A. Fromme
Mission Research Corporation
5434 Ruffin Road
San Diego, California 92123

1 January 1983

Final Report for Period 15 April 1978—31 October 1979

CONTRACT No. DNA 001-79-C-0083

APPROVED FOR PUBLIC RELEASE;
DISTRIBUTION UNLIMITED.

THIS WORK WAS SPONSORED BY THE DEFENSE NUCLEAR AGENCY
UNDER RDT&E RMSS CODE B323079464 R99QAXEE50224 H2590D.

DTIC FILE COPY

Prepared for
Director
DEFENSE NUCLEAR AGENCY
Washington, DC 20305

DTIC
ELECTE
JUL 11 1984
S B

84 05 16 002

UNCLASSIFIED

SECURITY CLASSIFICATION OF THIS PAGE (When Data Entered)

REPORT DOCUMENTATION PAGE		READ INSTRUCTIONS BEFORE COMPLETING FORM
1 REPORT NUMBER DNA 6212F	2 GOVT ACCESSION NO. ADA143012	3 RECIPIENT'S CATALOG NUMBER
4 TITLE (and Subtitle) ELECTRON CHARGING AND SGEMP STUDIES ON SATELLITE DIELECTRICS	5 TYPE OF REPORT & PERIOD COVERED Final Report for Period 15 Apr 78 - 31 Oct 79	
	6 PERFORMING ORG. REPORT NUMBER MRC/SD-R-112	
7 AUTHOR(s) J.D. Riddell V.A.J. van Lint B.C. Passenheim D.A. Fromme	8 CONTRACT OR GRANT NUMBER(s) DNA 001-79-C-0083	
9 PERFORMING ORGANIZATION NAME AND ADDRESS Mission Research Corporation 5434 Ruffin Road San Diego, California 92123	10 PROGRAM ELEMENT PROJECT TASK AREA & WORK UNIT NUMBERS Subtask R99QAXEE502-24	
11 CONTROLLING OFFICE NAME AND ADDRESS Director Defense Nuclear Agency Washington, D.C. 20305	12 REPORT DATE 1 January 1983	
	13 NUMBER OF PAGES 64	
14 MONITORING AGENCY NAME & ADDRESS (if different from Controlling Office)	15 SECURITY CLASS (of this report) UNCLASSIFIED	
	15a DECLASSIFICATION DOWNGRADING SCHEDULE N/A since UNCLASSIFIED	
16 DISTRIBUTION STATEMENT (of this Report) Approved for public release; distribution unlimited.		
17 DISTRIBUTION STATEMENT (of the abstract entered in Block 20, if different from Report)		
18 SUPPLEMENTARY NOTES This work was sponsored by the Defense Nuclear Agency under RDT&E RMSS Code B323079464 R99QAXEE50224 H2590D.		
19 KEY WORDS (Continue on reverse side if necessary and identify by block number) Spacecraft Charging Triggered Discharge SGEMP Teflon (Fluoroethylene Propylene) Dielectrics Kapton (Polyimide) Electron Radiation Solar Cell Cover Glass Spontaneous Discharges Thermal Control Paint		
20 ABSTRACT (Continue on reverse side if necessary and identify by block number) An experiment was conducted to measure the electrical response of satellite thermal control dielectrics when exposed to mono-energetic electron beams from 5-30 keV. Responses included SGEMP pulses when exposed to short (<100 ns) pulses of low energy X-rays (< 2 keV), and spontaneous discharges. Significant SGEMP enhancement was noted as a result of precharging, and is explained by a theory which includes low-energy secondary electrons which escape via lateral edge fields. Potential profiles were taken across the		

UNCLASSIFIED

SECURITY CLASSIFICATION OF THIS PAGE(When Data Entered)

20. ABSTRACT (concluded)

sample surface during charging and after discharges. Transient measurements included charge flowing from the substrate, charge "blown off" the test object, and between different portions of the substrate. Two anomalous events are reported which showed "blow-off" lasting up to a microsecond after photon exposure, accompanied by a late time substrate current.

UNCLASSIFIED

SECURITY CLASSIFICATION OF THIS PAGE(When Data Entered)

PREFACE

The authors wish to thank their colleagues W.N. Johnston, Pat Roach, and Norm Hall for mechanical and electrical construction, assistance with the experiment execution, and data acquisition. We thank Dale Shamblin of FCNNA for his assistance with the data acquisition, and the OWL II crew of the Physics International staff.

Accession For	
NTIS	<input checked="" type="checkbox"/>
CFARI	<input type="checkbox"/>
DTIC TAB	<input type="checkbox"/>
Unannounced	<input type="checkbox"/>
Justification	
By	
Distribution/	
Availability Codes	
Dist	Avail and/or
	Special
A-1	



TABLE OF CONTENTS

<u>Section</u>		<u>Page</u>
	PREFACE	1
	LIST OF ILLUSTRATIONS	3
1	INTRODUCTION	5
2	EXPERIMENTAL DETAILS	7
3	EXPERIMENTAL RESULTS	18
	3.1 POTENTIAL PROFILES	18
	3.2 TRANSIENT SIGNALS	32
	3.3 DELAYED SGEMP EMISSION	44
4	SUMMARY	48
	REFERENCES	50
	APPENDIX	51
	GLOSSARY OF TERMS	58

LIST OF ILLUSTRATIONS

<u>Figure</u>		<u>Page</u>
1	Picture of the test body showing traverse, sample and B sensors.	8
2	Top view of the SGEMP/SCC experiment chamber.	12
3	Schematic and electrical equivalent circuit of a dielectric disk on the end of a cylinder in a vacuum chamber.	16
4	Potential profile of a sample of thermal control paint pre-charged with 25 keV electrons at near normal incidence, before and after EWR exposure #4805 at 11:37 on 3/22/79.	20
5	Transient current flow from the test body to the metal backing of the fiberglass sample during EWR exposure #4805 at 11:37 on 3/22/79.	22
6	Surface potential profiles for a paint sample charged 10 min. with 30 kV electrons.	24
7	Surface potential profiles for a paint sample charged 10 min. with 30 kV electrons.	25
8	Teflon - Before and after photon shot 4812 and after time delay.	26
9	Kapton voltage profile charged for 7 min. with 20 kV electrons, before and after shot 4780 (horizontal traverses).	27
10	Kapton potential profile after charging for 7 min. with 20 kV electrons, before and after shot 4780 (vertical traverses).	28
11	Solar Cell Glass - 5 min charge at 20 kV.	30
12	Space chargin limiting.	34
13	Measurements of transient current flow to and from identical points on the same teflon sample exposed to nearly equal photon bursts with the sample (a) uncharged and (b) charged to $\langle V \rangle = 11 \pm 1$ kV.	35
14	Comparison of measured and calculated photoemission of paint exposed to an EWR source, illustrating the significant enhancement resulting from transverse fields sweeping low energy electrons away from the precharged dielectric.	36

LIST OF ILLUSTRATIONS (Concluded)

<u>Figure</u>		<u>Page</u>
15	Charge leaving substrate vs. dose.	38
16	Charge leaving substrate vs. pre-shot average voltage.	40
17	Charge leaving the test object vs. dose.	41
18	Charge leaving test object vs. pre-charged average voltage.	42
19	Charge leaving test object vs. charge leaving substrate.	43
20	Transient current record showing the prompt and delayed current component.	45
21	Test object voltage (10^3 V/div) versus time (200 ns/div).	46

SECTION 1 INTRODUCTION

This report presents the data from an experiment on spacecraft charging. The experiment consisted of exposing a test object covered with satellite dielectrics to 5-30 keV electrons, then exposing the charged dielectrics to a short, intense pulse of photons ($\bar{E} \approx 1.2$ keV) and measuring the electrical response. In conjunction with this experiment MRC performed another experiment which consisted of charging the dielectrics in a similar manner, observing the charging characteristics, but then continuing charging until the dielectrics discharged spontaneously.

It is known that external dielectrics on satellites become charged in space as a result of the natural radiation environment. It is also known that x-rays will produce emission of electrons from the surface of these dielectrics, creating a system generated electromagnetic pulse (SGEMP). Theory says that this SGEMP response should be much larger from dielectrics which have been charged before exposure to the photons. Exploding wire radiator (EWR) exposures of an electron-precharged Skynet Qualification Model satellite (Ref. 1) established that the SGEMP response was enhanced by precharging either the thermal paint or solar cell covers, and that on one occasion, a massive discharge of solar cell covers appeared to be triggered by the EWR exposure. The present experiment was designed to study SGEMP enhancement and discharge triggering under controlled and measured conditions, to provide data for comparison with theoretical calculations and to identify the causal parameters.

The results of the present experiment have been partially presented in Reference 2, which is attached to this report as Appendix 1. The

results of the simultaneous experiment on spontaneous discharges have been presented in Reference 3. Those data will be mentioned here only in comparison to the work with the photon pulses.

The EWR source produces a narrow (50-100 ns) fast risetime (≈ 10 ns) pulse of photons from exploding aluminum wires, resulting in emission of low energy photoelectrons from the dielectric samples (Ref. 4,5). This EWR source (OWL II at Physics International) has been used for previous SGEMP experiments on simple objects (Ref. 6), on a structural model of the Skynet satellite (Ref. 7) and on a simple model of a resonant structure (Ref. 8).

SECTION 2 EXPERIMENTAL DETAILS

The exterior geometry of the test structure is indicated in Figure 1. In all cases the dielectric samples were 82 cm in diameter, supported on an 85 cm diameter, 0.95 cm (3/8") thick Plexiglas disk. The samples were mounted on the front of a 120 cm diameter by 51 cm long aluminum cylinder. The dielectric materials investigated were:

- (1) Back-surface silvered Teflon, 82 cm (32 in) in diameter, and 0.013 cm (0.005") thick stretched over the Plexiglas disk.
- (2) Back-surface aluminized Kapton, 82 cm (32 in) in diameter, 0.013 cm (0.005 in) thick stretched over the Plexiglas disk.
- (3) Silicon alkyd white thermal control paint approximately 0.013 cm (0.005 in) thick applied to an 85 cm diameter fiberglass disk, approximately 0.035 cm (0.014 in) thick, on a segmented copper back plate. The segmented copper plate had a 27 cm diameter central disk surrounded by segmented rings (shown dotted in Fig. 1). This multi-layer structure was cemented to the Plexiglas disk.
- (4) A 50 cm × 50 cm array of 0.030 cm (0.012 in) thick MgF₂ coated fused silica solar cell cover slips obtained from Optical Coating Labs, Inc. (OCLI). These slips covered copper tape configured to electromagnetically simulate solar cells, on a 0.035 cm thick fiberglass sheet supported on the

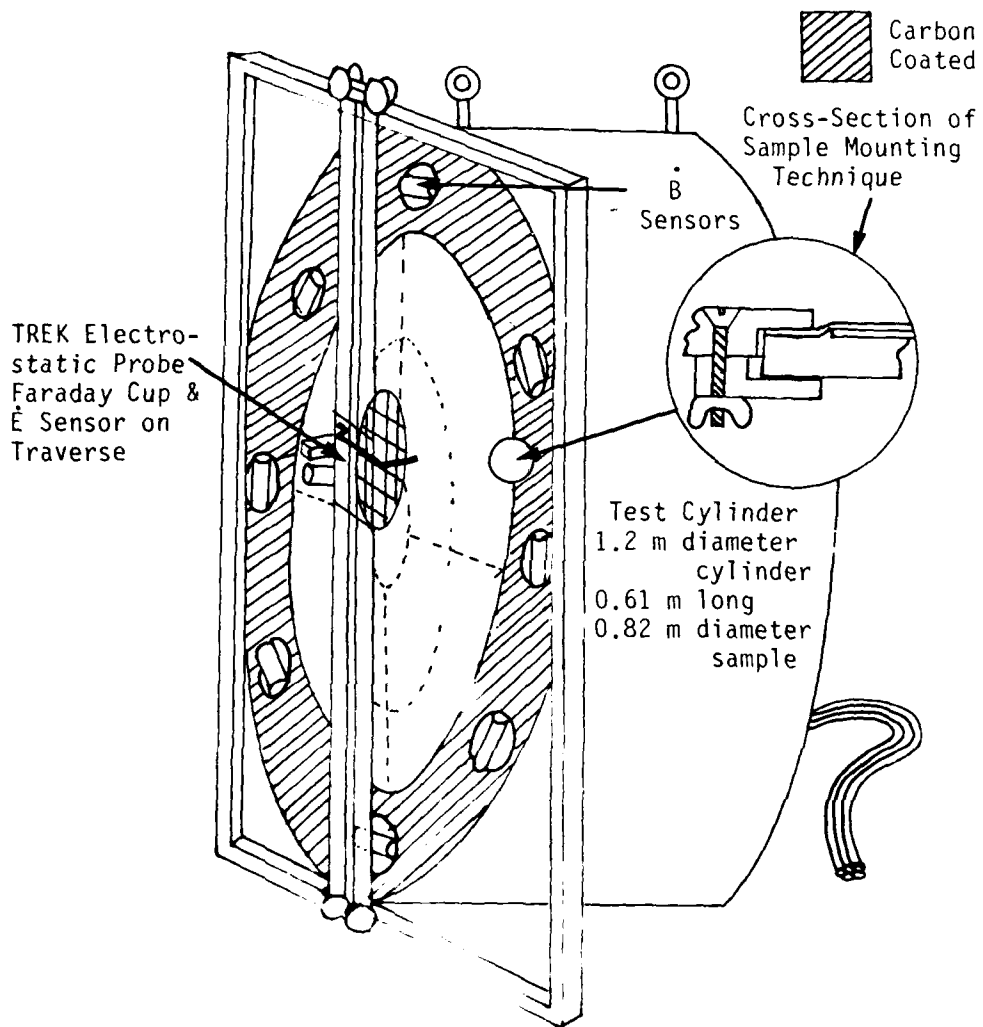


Figure 1. Picture of the test body showing traverse, sample and B sensors. Insert shows the way the sample was attached to the test body.

Plexiglas disk. The array was composed of both 2 cm x 2 cm and 4 cm x 4 cm cells. The spacing between cells (≈ 0.050 cm), conductor routing, and the interconnections of the copper tape were designed to mimic actual solar panel geometry as closely as possible.

Interconnect tabs on real solar cells are flat strips bent into the shape of an omega (Ω), to provide strain relief, which causes a conducting hairpin to extend above the surface of the cell cover. This physically small feature might appreciably alter the discharge characteristics of solar cell cover arrays, as it introduces a conductor in the plane of the surface charge. These interconnects were simulated over approximately ten percent of the array with short pieces ($\approx 1/8$ in) of 0.050 cm (0.020 in) diameter wire soldered to the copper tape between adjacent cell covers. Other areas of the array were without simulated interconnect protrusions. No difference was noted. Cell covers and copper tape were intentionally deleted from a few portions of the array (1) to simulate areas near penetrations, and (2) to provide a sufficient area to reliably measure fiberglass surface potential with an electrostatic voltmeter.

For comparison purposes, the range of a 30 keV electron is about 20 μm in plastic, the absorption depth of a 1 keV photon is 5 μm and that of a 2 keV photon is 30 μm . The samples were all at least 125 μm thick.

The dielectric samples were surrounded by eight \dot{B} or surface current sensors (EG&G model CMLX3B) oriented to detect radial current flow (schematically indicated in Fig. 1).

The magnitude and time history of spontaneous discharge were measured with EG&G \dot{B} surface current probes, or by measuring currents from the cylinder to the conducting substrates of the samples with Tektronix CT-2 current transformers. In the cover glass array and thermal control paint samples, information about charge redistribution within the dielectric (as opposed to blow-off and punch-through) was inferred from currents flowing

between the segmented metal substrates. These currents were also measured with current transformers.

Fast transient data were transmitted to the recording instrumentation through HDL/DNA 400 MHz fiber optic data links, recorded on Tektronix 7912 transient digitizers, and processed on a PDP/1140 computer.

The test cylinder was connected to instrumentation ground through a 50 k Ω resistor chain. This kept the cylinder potentials to less than 0.5 V during charging at measured current densities of $\approx 10^{-9}$ A/cm². However, the RC time constant of this resistor string and cylinder capacitance to the tank (≈ 240 pf) was calculated to be about 12 μ s, so the test structure was effectively isolated during spontaneous discharges and EWR photon pulses, which generally last less than 0.1 μ s (FWHM).

As shown in Figure 1, the front of the cylindrical test object was surrounded by a square frame which supported small motors, pulleys and belts (not shown) to drive a traverse carrying the probe of a TREK noncontacting electrostatic voltmeter, a Faraday Cup, and an \dot{E} sensor, over the surface of the sample. The spatial resolution of the electrostatic voltmeter is estimated to be ± 3 mm, and the Faraday Cup area was approximately 1 cm². The \dot{E} probe was used as an oscilloscope trigger in spontaneous discharge studies. Both the traverse frame and aluminum ring surrounding the dielectrics were coated with colloidal graphite to (1) inhibit dielectric charging, and (2) minimize photoelectron emission from the aluminum.

An expanded inset in Figure 1 indicates how the samples were held in the cylinder. The samples, supported on 3/8 in thick plastic disks, were inserted through the removable aluminum back of the test cylinder and clamped in a ring cut in the back of the front face. Thus, the truly flat samples (Teflon and Kapton) were recessed 0.25 cm (0.100 in) below the front aluminum ring. The edge of the aluminum ring touching the dielectric had been machined and finished using typical machine shop practice. The edge of

this ring had been "broken", that is, the sharp edges from the cutting operation had been softened with a fine file or sandpaper to produce a corner with a radius of curvature on the order of 0.025 to 0.050 cm (0.010 to 0.020 in).

Figure 2 shows the experiment's overall test geometry. The test cylinder was suspended very nearly in the center of the 3 m diameter, 3.6 m long vacuum tank. Since the object hung on nylon ropes from a rotary feed-through, it could be rotated about a vertical axis passing through the cylinder center, along a diameter "in situ" to point in any direction. Non-normal orientations permitted investigations of the effect on the surface potentials of charging at non-normal angles. The vacuum chamber was lined with two cylindrical layers of 200 Ω /square carbon-coated cloth to damp chamber EM resonances. The dampers were nominally located at 80 and 90 percent of the tank diameter, and were open at each end.

Photon time histories and shot-to-shot fluence variations were monitored with four (300V) biased fast diodes previously discussed in Reference 5. These 50 Ω diodes were mounted near the back wall of the chamber and were hardwired to Tektronix 7904 scopes with copper-jacketed 50 Ω coaxial cable. Two diodes were gold, one was glass, and one was paint. The photoelectron emission of gold exposed to the EWR source has been studied by MRC and others (Ref. 4). The glass and paint photodiodes served to define the photoelectron emission relative to gold. Because these diodes were located in the periphery of the electron gun emission pattern, it is not likely that they reached the same surface potential as the test material except in cases where the sample was charged for extended periods. Nevertheless, enhanced emission from precharged dielectrics was clearly observed.

During the course of the experiment, two 0-30 kV electron guns were employed. These guns were located symmetrically on either side of the EWR port. One was a flood gun, described in Reference 6, constructed for DNA by IRT Corporation. Faraday Cup measurements indicated that this gun

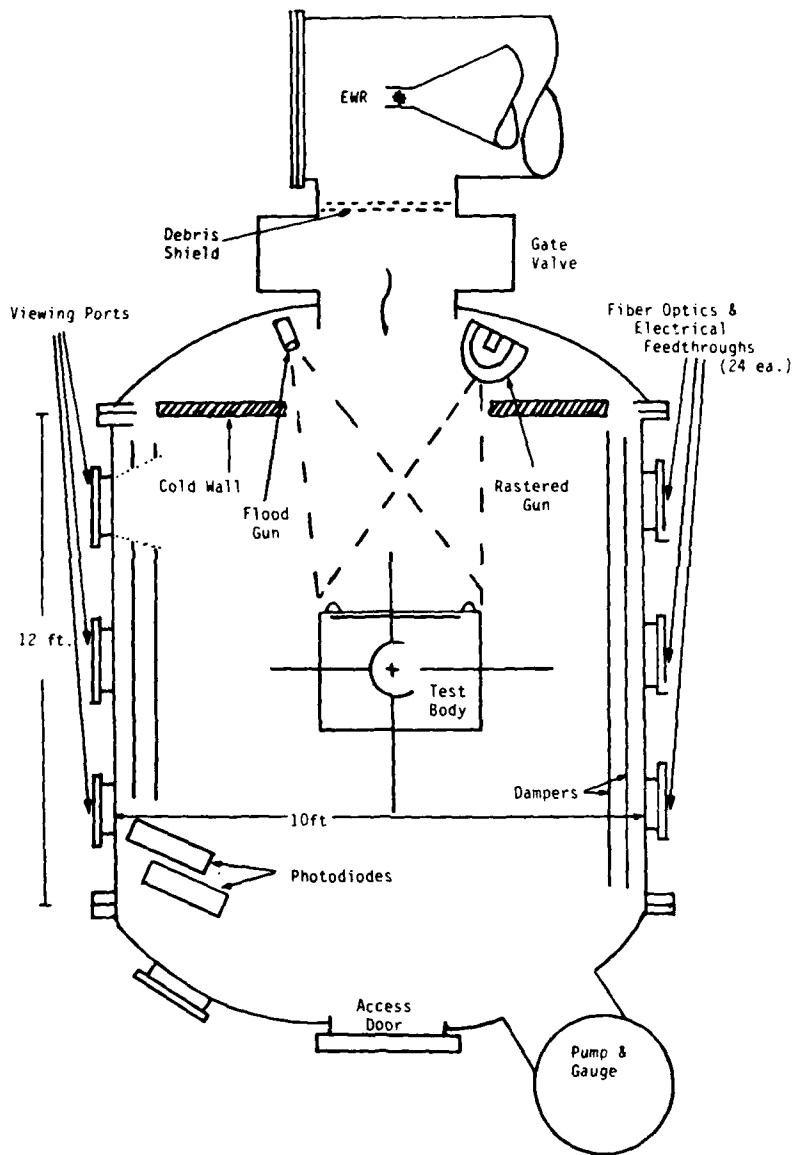


Figure 2. Top view of the SGEMP/SCC experiment chamber.

provided illumination which differed by less than a factor of two from the center to the edge of the sample. Acceleration potential was determined by floating the gun filament supply to a negative potential with respect to a fine wire grid with a controlled high voltage supply. Gun current was regulated with a feedback circuit which sensed gun emission current and modulated the filament supply power. The other (rastered) gun was constructed by MRC/SD and was designed to illuminate the sample with a small diameter (≈ 2 cm diameter) spot. This gun was constructed from an electrostatically focused and deflected cathode ray tube gun. Potential and current were controlled as with the flood gun. For equal total gun current, the instantaneous beam current density was approximately 1600 times larger in the focused beam as it swept across the sample. Comparable potential distributions were produced with comparable total electron fluences from either gun on all four materials. This indicates the charge build-up is not particularly sensitive to instantaneous beam current densities over a range from approximately 10^{-10} A/cm² to $\approx 10^{-6}$ A/cm.

The chamber was evacuated with a liquid nitrogen trapped silicone oil diffusion pump and a mechanical roughing pump. In addition there was a liquid nitrogen cold wall in the tank. The tank pressure normally ranged from about 2 to 5×10^{-6} torr. Rapid discharge (approximately 10^3 volts/s) of all charged insulators was observed at $\approx 2 \times 10^{-4}$ torr. This discharge was accompanied by a flash of light and a temporary reduction in pressure. From Paschen's gas discharge curve, one would expect rapid discharge of surfaces charged to $\approx 10^4$ V and separated by more than 10 cm at approximately 2×10^{-4} torr. At pressures below $\approx 1 \times 10^{-4}$, it was determined for that samples charged to 10 to 16 kV, the sample potential decayed at a rate of 20 to 70 V/min. Assuming the principal charge loss mechanism was conductivity through the sample as opposed to air ionization, we inferred bulk resistivities of 10^{17} to 10^{18} ohm-cm for Kapton and Teflon, and 10^{16} to 10^{17} ohm-cm for paint and cover glasses. However, as we showed in Reference 3, these conductivities are dependent on charging conditions and time after the end

of electron exposure, even though the conductivity is beyond the electron "range".

A 1 m diameter gate valve separated the EWR source from the test chamber between shots, when the source chamber was vented to change wires. A 70 percent transmitting copper screen and .002 cm Kapton debris shield protected the test chamber vacuum from the pressure pulse in the source chamber which accompanies the photon pulse.

The test chamber was continuously monitored. Occasionally, the debris shield was ruptured or punctured at shot time and the chamber pressure would rise to $\approx 3 \times 10^{-4}$ torr. On shots where the debris shield retained integrity, the pressure never exceeded $3 - 5 \times 10^{-5}$ torr. A comparison of the pre-to-post shot potential (charge) profile was considered valid only when the pressure remained below 1×10^{-4} torr. However, even when the debris shield was compromised and the pressure ultimately exceeded 10^{-4} torr, the fast transient data is still valid since the measurements were completed (≈ 100 ns) long before the sample was exposed to the pressure surge (≈ 1 ms).

Samples were handled with gloves with more-than-normal care, but were unavoidably exposed to laboratory atmosphere for several weeks prior to testing. Close, careful visual examination of the reflecting Kapton samples after several days of tests revealed traces of vacuum pump oil. Subsequently, all samples were washed with reagent grade ethyl alcohol after installation and before pumpdown.

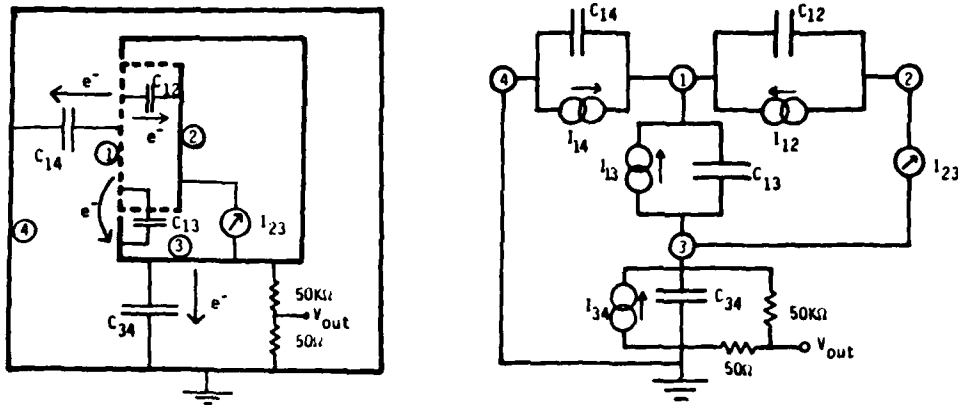
Summarized briefly, the experiment went as follows: electrons from the electron gun are buried a short way into the dielectric. As charge continues to accumulate, the potential at the front surface rises, as does the field between the embedded charge and the metal substrate. If the charging continues long enough, the dielectric will discharge spontaneously. Before that happened, we exposed the charged dielectric to the x-ray

pulse. The x-rays produce some "primary photo-electrons" in the 0-2 keV range, which in turn produce large numbers of "secondary electrons" in the 0-50 V range. These electrons then can leave the test object, i.e., "blow-off", or rearrange themselves on the test object. This charge motion is what generates the SGEMP signal.

Figure 3 represents the electrical equivalent circuit of this experiment, where node 1 is the trapped electron charge layer, node 2 is the metal film on the back of the dielectric, node 3 is the test cylinder and node 4 is the vacuum chamber. Current generator I_{12} represents a "punch-through" current through the dielectric sample. I_{13} represents the charge transfer from the dielectric to the test cylinder ("edge" current). I_{14} represents "blow-off" from the dielectric to the vacuum chamber walls. I_{34} represents charge emission from the test cylinder to the vacuum chamber walls. I_{23} is the current between back plate of the sample and the test cylinder, actually measured with a Tektronix CT-2 sensor and is influenced by blow-off, edge, and punch-through currents. I_{23} will later be referred to as I_{total} . V_{out} , 0.1% of the voltage of the test cylinder above the vacuum chamber, is proportional to blow-off currents, I_{14} and I_{34} , minus the punch-through current scaled down by the capacitance ratio $(C_{14} + C_{34})/C_{12}$. Distinguishing between charge emitted to infinity (blow-off) and charge which is returned to the body is very significant because the coupling or ability to produce SGEMP by blow-off is much greater than by flash-over or punch-through.

The indicated capacitances are self-explanatory. They are estimated to be: $C_{13} \approx 40$ pf, $C_{14} \approx 100$ pf, $C_{34} \approx 60$ pf. C_{12} is estimated to be around 70 nf for Teflon and Kapton, 20 nf for paint and 15 nf for glass.

From the equivalent circuit, we determine the following equations relating the currents and capacitances:



- ① = Charge layer on dielectric
- ② = Metal substrate
- ③ = Test body
- ④ = Vacuum tank

Figure 3. Schematic and electrical equivalent circuit of a dielectric disk on the end of a cylinder in a vacuum chamber.

$$\begin{aligned} \text{Node 1: } \quad & \dot{V}_1 (C_{12} + C_{13} + C_{14}) + \dot{V}_3 (-C_{12} - C_{13}) \\ & = I_{12} + I_{13} + I_{14} \end{aligned}$$

$$\text{Node 2: } \quad \dot{V}_1 (-C_{12}) + \dot{V}_3 (C_{12}) - I_{23} = -I_{12}$$

$$\text{Node 3: } \quad \dot{V}_1 (-C_{13}) + \dot{V}_3 (C_{13} + C_{34}) + I_{23} = -I_{13} + I_{34}$$

(note that $V_2 = V_3$)

The change in V_3 (later referred to as V_{body}) was recorded by a Tektronix 7904 oscilloscope. The change in $(V_1 - V_3)$ can be determined by comparing TREK potential profiles before and after discharge (where available). As noted above, I_{23} was measured directly and called I_{total} .

SECTION 3 EXPERIMENTAL RESULTS

The data for each material can be divided into two categories: (1) potential profiles (taken with the TREK non-contacting electrostatic voltmeter to determine the charged condition of the sample), and (2) fast transient digitizer computer plots (from Tektronix 7912 digitizers) and oscilloscope pictures of the transient reponse of V_{body} .

3.1 POTENTIAL PROFILES

Through all stages of the experiment, the TREK probe was used to sweep across the samples to give an idea of where and how much charge was distributed on the dielectric surface. An effort was made to determine the condition of the entire sample before and after photon exposures. These amounted to what we refer to as "picture frames": sweeps near the top, near the bottom, near the left side, near the right side; or "Tic-tac-toe patterns": "picture frames" plus a sweep across the horizontal center line and vertical center line. A tic-tac-toe pattern leaves squares around 20 cm by 20 cm uncovered, but since each sweep took one minute or more, the sample could have changed significantly from the beginning to the end of a pattern if any more sweeps had been included. The voltmeter averages over an area of about 3 mm radius. The location of the sweep is accurate to within ± 5 mm. The scale locating the probe along the sweep is uncertain to $\approx 5\%$. This uncertainty is largely due to our computer digitizing process and can be compensated for by merely shifting sections of the traces when comparing two or more.

An effort was made to observe the status of the potential on the samples during the charging process. This effort has been reported in Reference 3.

It had been hoped before the test series, that the potential profiles before and after the photon exposures could be compared, the amount of charge which had left the surface of the sample determined, and that charge compared with the charge transfer recorded as transient signals. Unfortunately, this could not be accomplished because the time between the last sweep and the photon shot was large (15-60 min), allowing for substantial charge leakage in the interim, while the charge moved by the photons was quite small. Nonetheless, we gained considerable useful information from the potential profiles.

For example, Figures 4a and 4b show a three-dimensional representation of the measured potential (charge) profile on the paint sample before and after OWL II shot #4805 executed at 11:37 on 03/22/79. The average potential profile before the shot is 16 ± 1 kV with peak potentials of 20 kV. The average potential after the shot is 12.5 ± 1 kV with peak potentials of 16 kV. This sample had been charged with 25 kV electrons at nearly normal incidence. Notice that the potential (charge) profile has considerable structure. Although this short range structure is characteristic of the sample rather than the source and was observed for all sample types, it is only partially reproduced on successive charging. The structure is apparently representative of differences in deposited charge rather than differences in capacitance of the sample, since the thickness of the samples are quite uniform and presumably constant with time. This leads us to believe that it is due to either differences in conductivity through the sample, or in secondary emission coefficients. We can imagine that either of these could change with each discharge of the sample, whether induced by photons, a pressure increase, or spontaneously induced. Reference 10 shows how the charging characteristics of Teflon were significantly altered by a discharge.

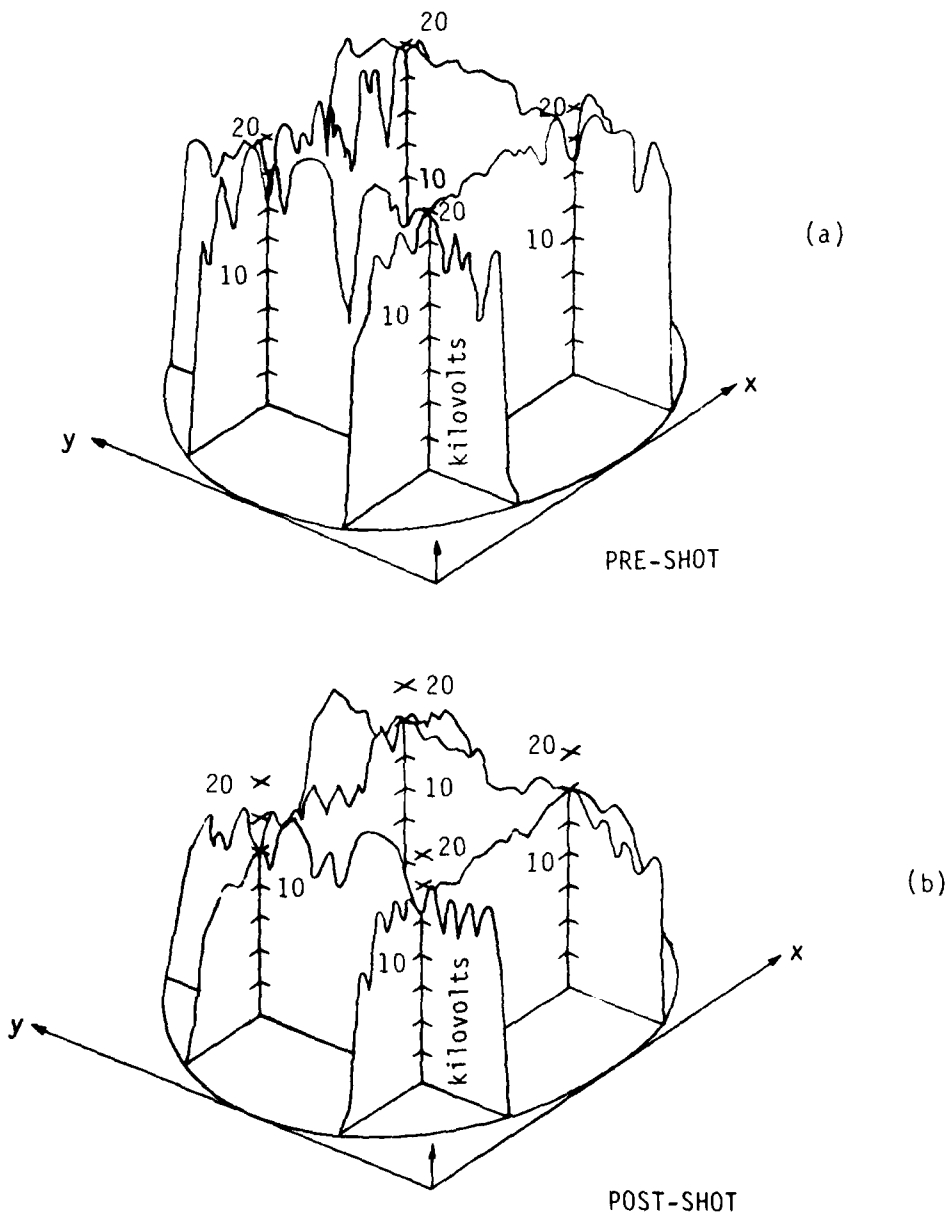


Figure 4. Potential profile of a sample of thermal control paint precharged with 25 keV electrons at near normal incidence, before and after EWR exposure #4805 at 11:37 on 3/22/79.

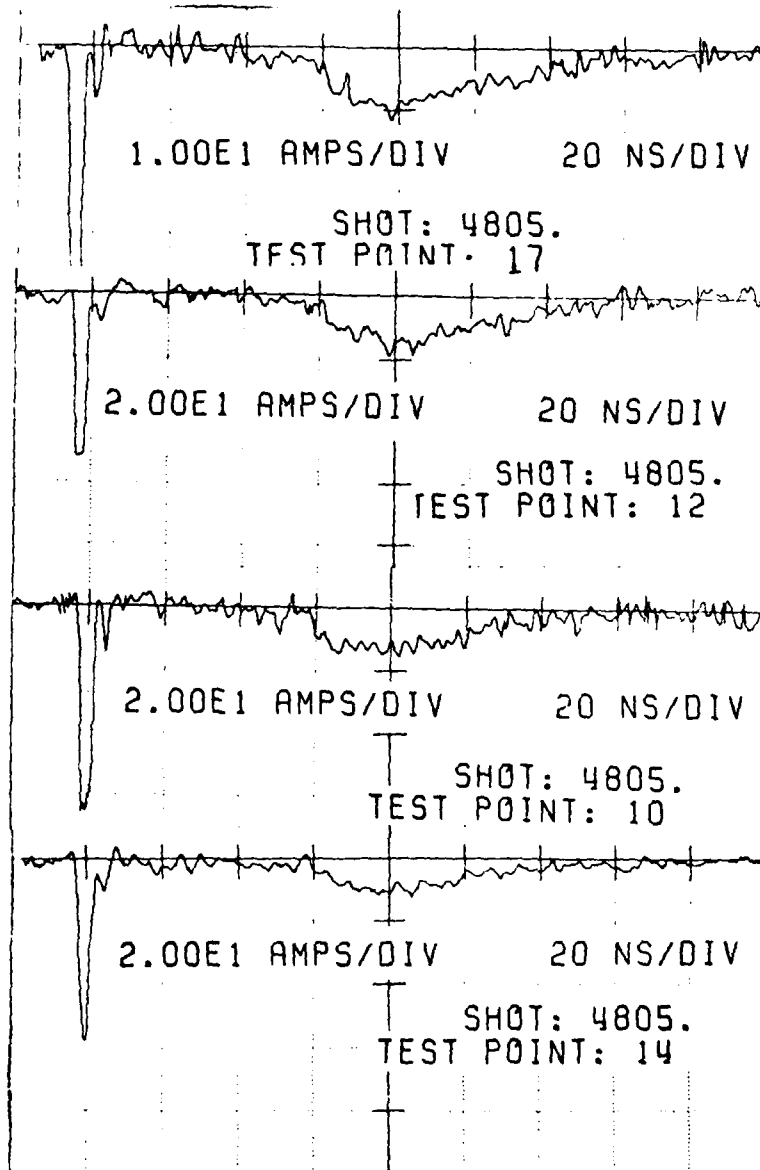
The pre-shot profile in Figure 4 was taken 55 ± 5 min before the shot. The post-shot profile was taken between 5 and 10 min after the shot. For 30 min immediately after the pre-shot profile measurements, the potential at one selected point was monitored. From this measurement, we found the potential leaked away at a rate of 70 ± 5 V/m. The measured capacitance from the sample surface to the metal backplate is approximately 20 nf. The pre- and post-shot voltage profiles indicate a net charge loss from $\Delta Q = C\Delta V$ of $2 \times 10^{-8} \times 4 \times 10^3 = 80 \mu\text{C}$, which is almost entirely accounted for by the static charge loss $\Delta Q = C \frac{dV}{dt} \Delta t = 20 \text{ nf} \times 55 \text{ V/min} \times 55 \text{ min} \approx 80 \mu\text{C}$. Successive traverses over the same area show that the potential sags fairly uniformly. This is what one would expect, since except for a band approximately 1 mm thick around the periphery of the sample, the field is primarily directly through the thin dielectric. Under these circumstances, the potential loss rate implies dielectric (paint and fiberglass resistivity) of $\rho = VA/Cd(\Delta V/\Delta t) \approx 5 \times 10^{16}$ ohm cm. Figure 5 is a composite of the measured transient currents to the backplate during the shot. The integral of these currents is

$$\Delta Q = \int_0^{\infty} I(t)dt = 1.5 \mu\text{C}.$$

Furthermore, these measured currents include both the charge that flows from the dielectric to the metal test object as well as the charge blown off to infinity. One can infer the fraction of charge blown off from the potential obtained by the test object. In this particular case, the test object rose to approximately 1 kV, which implies that only $Q = C\Delta V = 0.24 \mu\text{C}$ actually escaped the test object.

Finally, notice that the potential minimum noted prior to the exposure (see Fig. 4a) is definitely absent after the EWR exposure. This is one of numerous examples of charge redistribution. In this particular case, a charge transfer of $\approx 1.6 \mu\text{C}$ is required to change the potential of a 10 cm wide valley by ≈ 4 kV.

FIDUCIAL MARK



MAR. 22, 1979

11:36:21

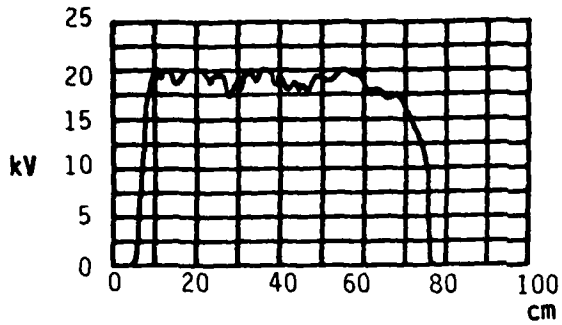
Figure 5. Transient current flow from the test body to the metal backing of the fiberglass sample during EWR exposure #4805 at 11:37 on 3/22/79.

It is worth mentioning that during the course of the experiment there occurred charge transfers of up to 500 μC during spontaneous discharges. However, for this geometry, at most approximately 3 μC could be discharged to the vacuum chamber walls (blown off) because the removal of that amount of charge would raise the body potential to such an extent that no further charge could be expelled. The rest of the charge had to move from one portion of the test object to another.

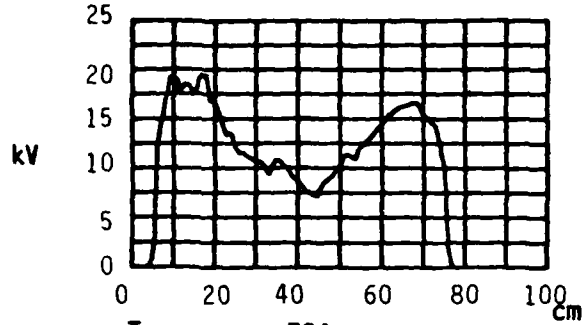
Figures 6 and 7 show the profile before and after the next photon shot, #4806, respectively. In Figure 6, the flat tops at 20 kV represent the maximum TREK range, but we can easily interpolate to get a reasonable estimate of the condition of the sample before the shot. After the shot, we see that in the center of the sample the potential has dropped ≈ 4 kV more than the general voltage sag, over an area ≈ 30 cm in diameter. This represents ≈ 30 μC of charge leaving the sample. But the transient measurements only indicate ≈ 1.5 μC leaving the sample, with ≈ 300 nC leaving the test object. Evidently the rest of the charge either went through the sample as a punch-through, or left before or after the the sweep of the instruments (≈ 2 μs), or left slowly, with small currents for long times.

Figure 8 shows that photon shot #4812 had little effect on the Teflon sample. The transient signals indicate ≈ 500 nC moved from the sample to the test object, and 80 nC left the test object. Note that a small valley at $x = 22$ cm becomes a peak after the shot and then becomes a local minimum again 20 minutes later. This effect appears to be outside the range of the probe position uncertainty if the lateral structure perpendicular to the sweep direction is comparable in size to that measured along the trace (≈ 2 cm).

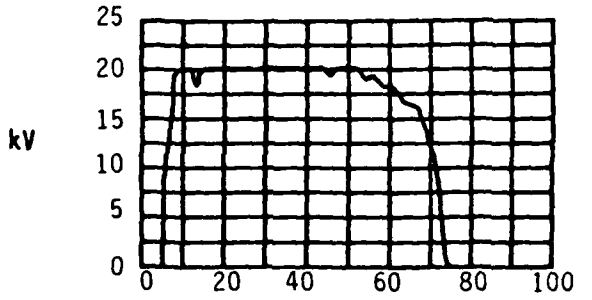
Figures 9 and 10 give another example of a photon shot which produced an insignificant change in the potential on the sample. In this case the material was Kapton, and the shot moved 220 nC, most of which probably



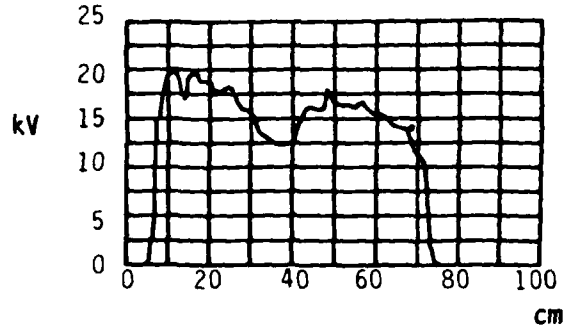
Traverse: 720
 x at y=56 cm
 (near top of sample)



Traverse: 724
 x at y=56 cm
 (near top of sample)

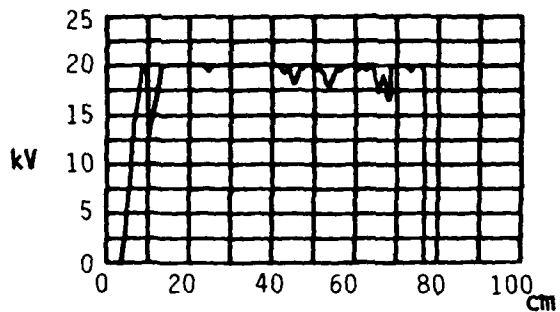


Traverse: 718
 x at y=20 cm
 (near bottom of sample)

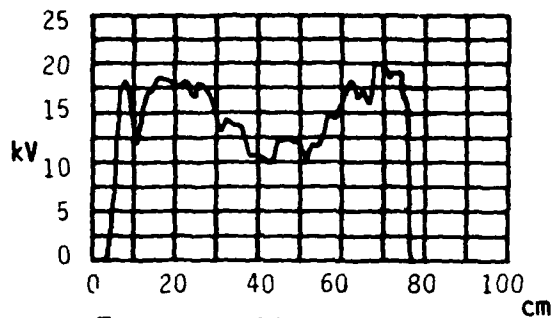


Traverse: 722
 x at y=20 cm
 (near bottom of sample)

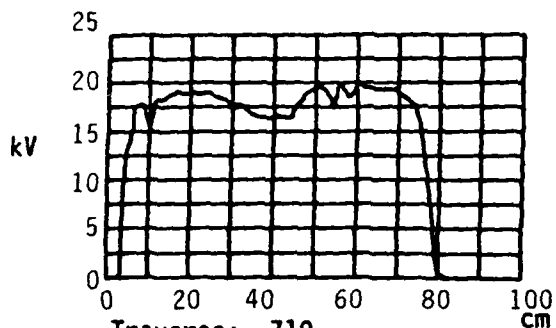
Figure 6. Surface potential profiles for a paint sample charged 10 min. with 30 kV electrons. These are horizontal traverses 10 min. after charging 35 min. before shot 4806 and a few minutes after shot 4806.



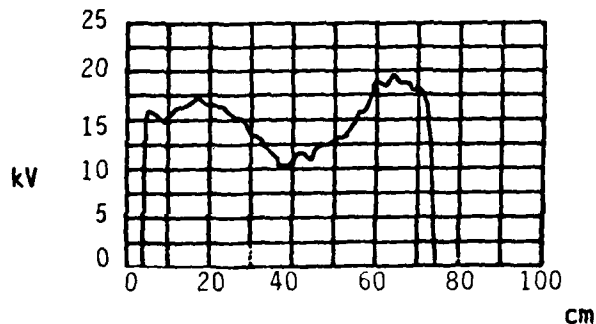
Traverse: 721
y at x=24 cm
(up left side of sample)



Traverse: 725
y at x=24 cm
(up left side of sample)

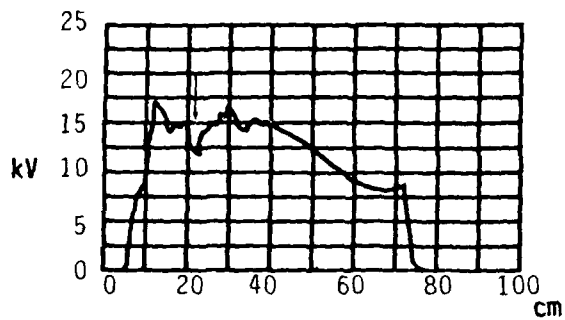


Traverse: 719
y at x=56 cm
(up right side of sample)

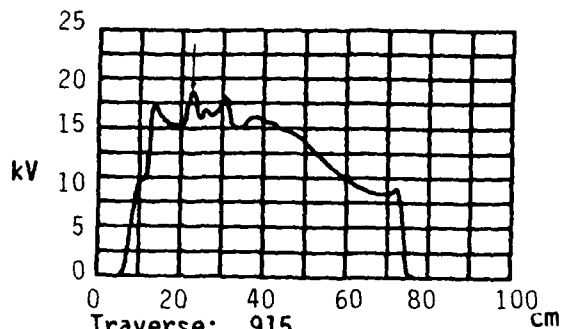


Traverse: 723
y at x=56 cm
(up right side of sample)

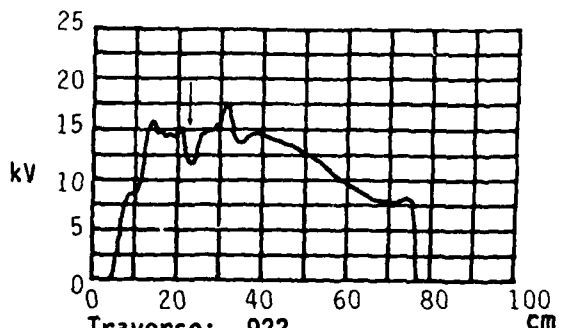
Figure 7. Surface potential profiles for a paint sample charged 10 min. with 30 kV electrons. These are vertical traverses 10 min. after charging 30 min. before shot 4806 and a few minutes after shot 4806.



Traverse: 909
 Charge: 90 sec. at 22 kV
 after spont. discharge



Traverse: 915
 Photon Shot: 4812
 20 min. after Tr. 909



Traverse: 922
 Time delay: 20 min. after Tr. 915

Figure 8. TEFLON - Before and after photon shot 4812 and after time delay. $V(x)$ traverses at $y = 20$ cm (near bottom of sample).

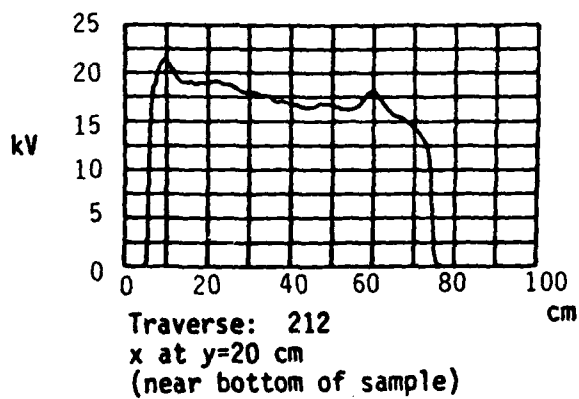
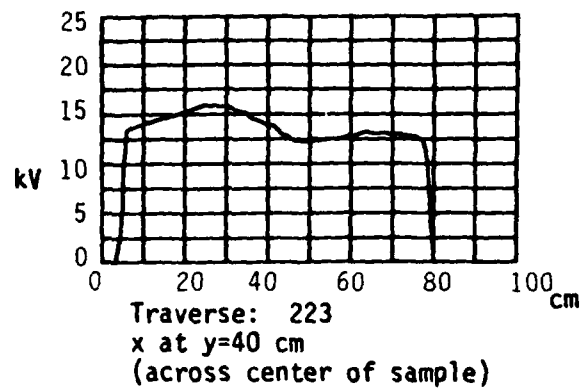
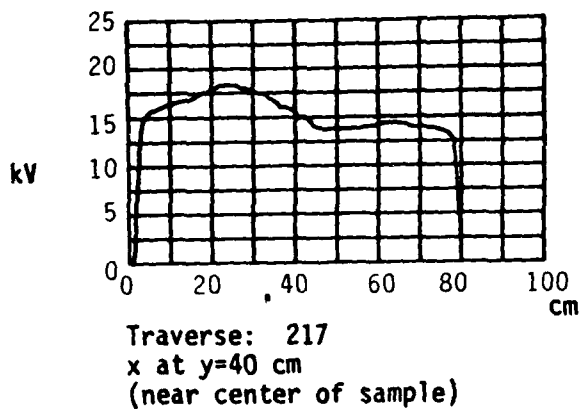
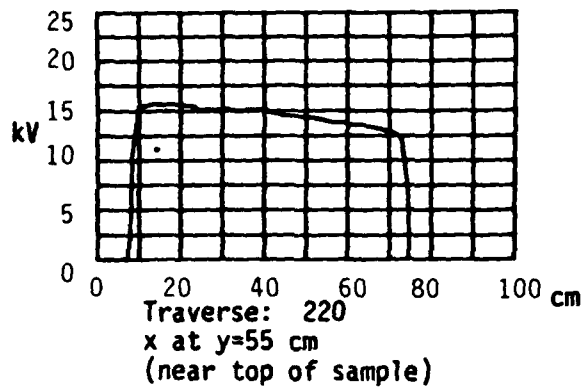
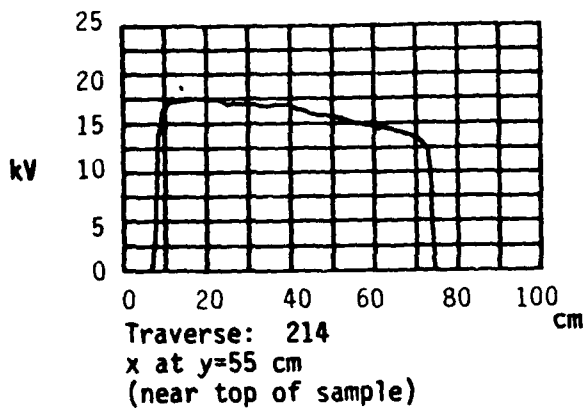


Figure 9. Kapton voltage profile charged for 7 min. with 20 kV electrons, before and after shot 4780 (horizontal traverses).

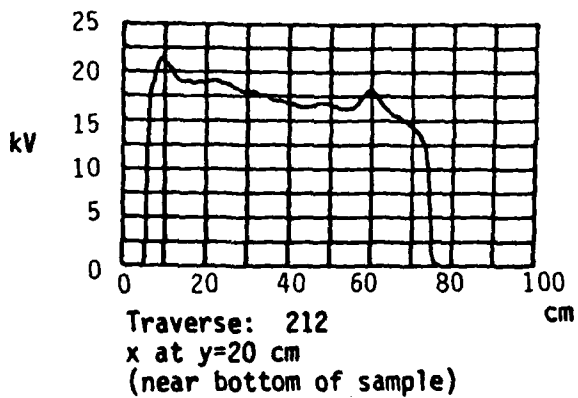
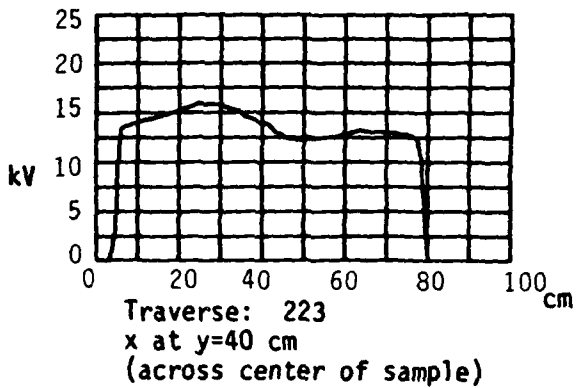
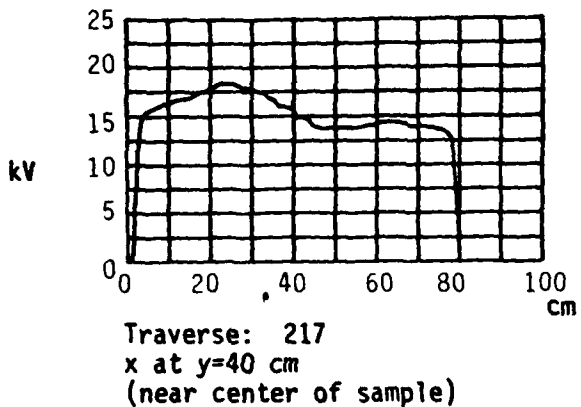
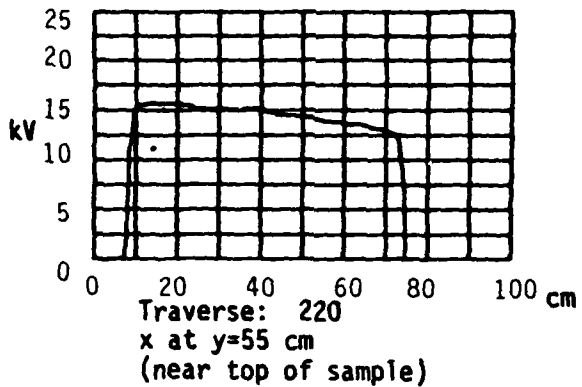
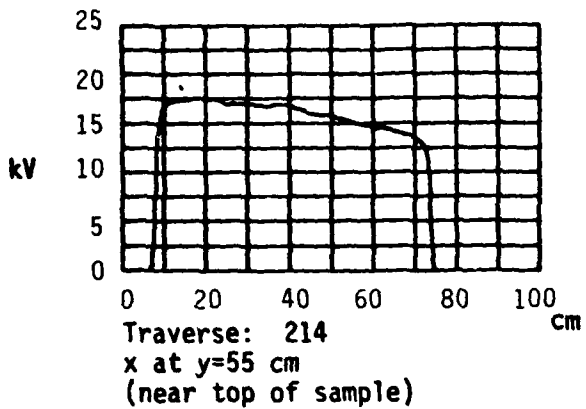


Figure 9. Kapton voltage profile charged for 7 min. with 20 kV electrons, before and after shot 4780 (horizontal traverses).

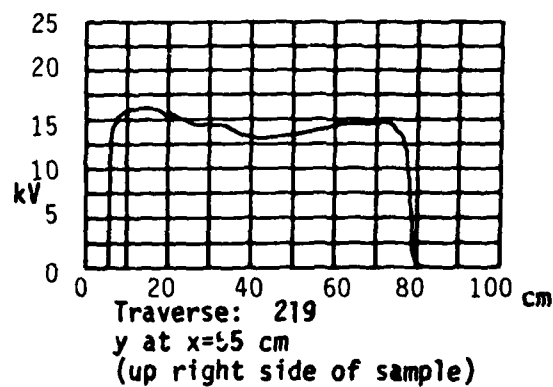
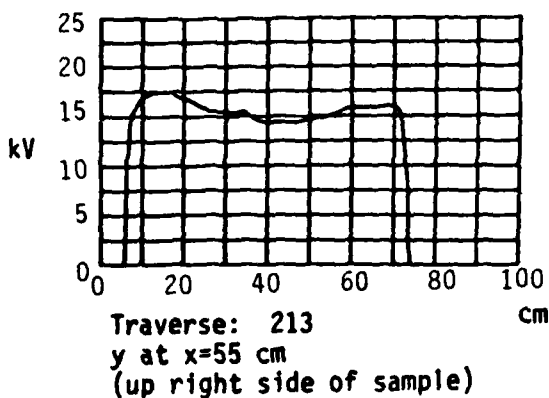
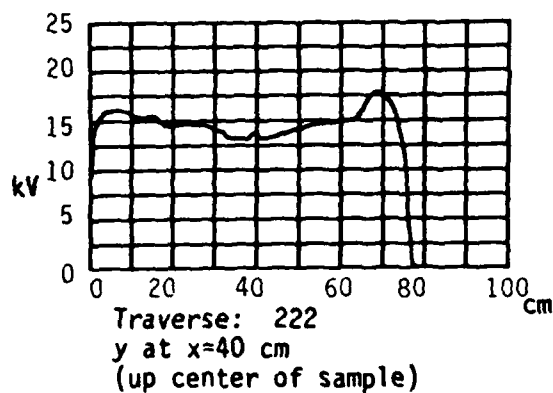
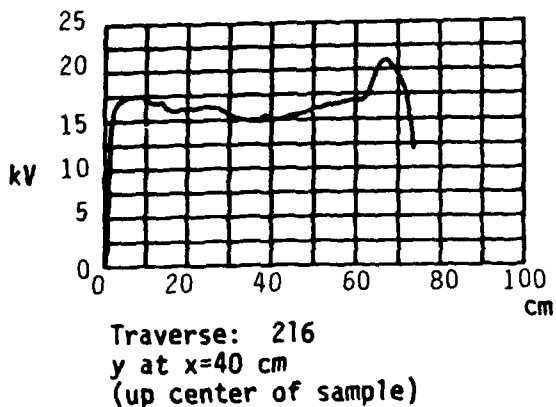
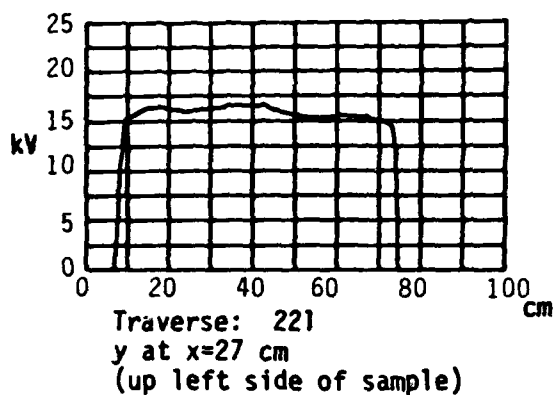
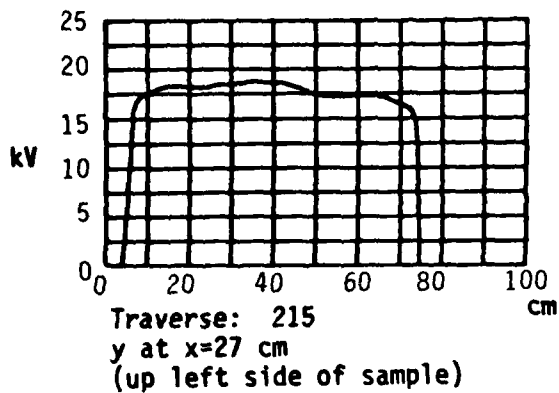


Figure 10. Kapton potential profile after charging for 7 min. with 20 kV electrons, before and after shot 4780 (vertical traverses).

left the test object. That amount of charge would only change the potential of the surface of the sample by a few volts compared with the test object, but it did raise the potential of the test object by ≈ 1 kV at the time of the shot.

We have included Figure 11 as an example of the potential profile for the solar cell cover glass panel. This figure gives an idea of the enormous amount of structure achieved on the panel. Between each cover glass there was a small 0.05 cm (0.020 in) exposed area of grounded copper tape, and surrounding the cover glasses was an area of fiberglass. As can be seen especially in Traverse 513, the fiberglass generally charged to considerably higher potential than the cover glasses. This was in part because the glass began having frequent spontaneous discharges at above 9 kV.

This solar panel "mock-up" was made to substantiate a model which is still in consideration to explain the "triggered" discharge on the Skynet Qual Model satellite. The hypothesis goes as follows:

"In the previous test on Skynet Qualification Model, electron precharging produced a potential profile with several gradients. Solar cells remained at or near ground potential, cover glass surfaces climbed to 10-12 kV before they spontaneously discharged; but fiberglass or thermal control paint in the vicinity of the solar cell cover glasses may have reached potentials in excess of 20 kV. The surface potential of the Qual Model was not measured extensively because the object was geometrically too complex. When the EWR burst occurred, charge was emitted from all exposed surfaces. Some charge was driven to infinity, some charge was collected by nearly low potential conducting surfaces, and some charge was transferred from the local high

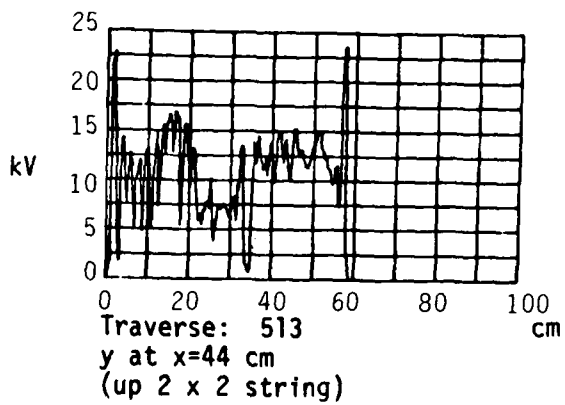
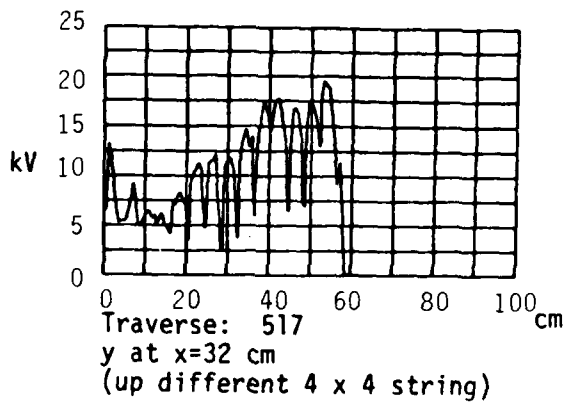
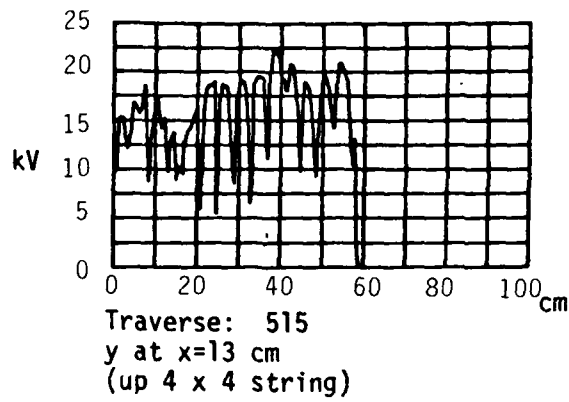


Figure 11. SOLAR CELL GLASS - 5 min charge at 20 kV.

potential ($V > 13$ kV) fiberglass to the comparatively low potential ($V \approx 9$ kV) coverslip. The exposed interconnects in a solar cell array are miniscule (10^{-2} cm²) compared to the exposed area of the glass surfaces (4 to 16 cm²). From measurements previously described, we know photocurrents of up to 10^{-2} A/cm² were emitted by EWR exposure, and only 10 to 20 percent actually escaped the body, the remainder returning to the object. Consequently, it is reasonable to hypothesize that a significant fraction of the charge emitted from the precharged dielectric surrounding and interspersed with the cover glass was collected on the glass. During the event, while the cover glasses and substrates were immersed in a sea of free charge, the potential gradients were insufficient to cause spontaneous discharge. However, as the sea of free charge dissipated, the coverslips found themselves charged to potentials greater than that required for spontaneous discharge. Enhanced emission from a precharged object set up conditions which cannot be induced by precharging alone. Such a hypothesis provides a feasible explanation for the singular but well documented triggered discharge observed in the Skynet tests (Ref. 8). It suggested that the failure to reproduce this effect in the most recent test series may be due to having an incorrect mix of high and low potential dielectrics, and furthermore suggests that the potentially serious triggered discharges might be controlled by minimizing the amount and/or proximity of high potential dielectrics in the vicinity of the solar array." (Ref. 2)

Although later calculations have modified many of the details of this model, the fundamental concept of charge liberated from a highly charged dielectric being deposited on a less negatively charged dielectric and overstressing the latter to breakdown, is still considered to be a likely explanation for the observation on the Skynet Qual Model.

3.2 TRANSIENT SIGNALS

On each photon shot, there were two primary transient measurements of interest: the current flowing between the substrate beneath the dielectric and the test object (I_{total}) and the change in voltage of the test object (V_{body}). The latter is proportional to the charge which left the body (blow-off): $\Delta Q = C\Delta V$, where C is the capacitance between the test object and the vacuum tank.

As the photons strike the dielectric, they lose energy to the release of photo-electrons. These electrons are referred to as "primary" electrons, and are born with energies close to the energy of the initial photons (1-2 keV). At most one primary electron is released for each photon. As the primaries pass through the dielectric they lose energy, so that the primary electrons emitted from the surface have a spectrum of energies from the photon energy down. As the primaries pass through the dielectric, the energy loss mechanism at work on them is that they in turn release "secondary" electrons with energies of 50 V or less. The "secondaries" born within a very short distance of the surface may escape the surface. The number of secondaries emitted from the surface can be large compared with the number of primaries emitted. Once outside the dielectric, the electrons, both primary and secondary, feel the influence of the positive image charges they left behind, and are attracted back toward the surface. If there is an external field outside the dielectric tending to draw the electrons away from the surface, then some of the electrons will be drawn away and some will return to the surface. The maximum current which can be drawn

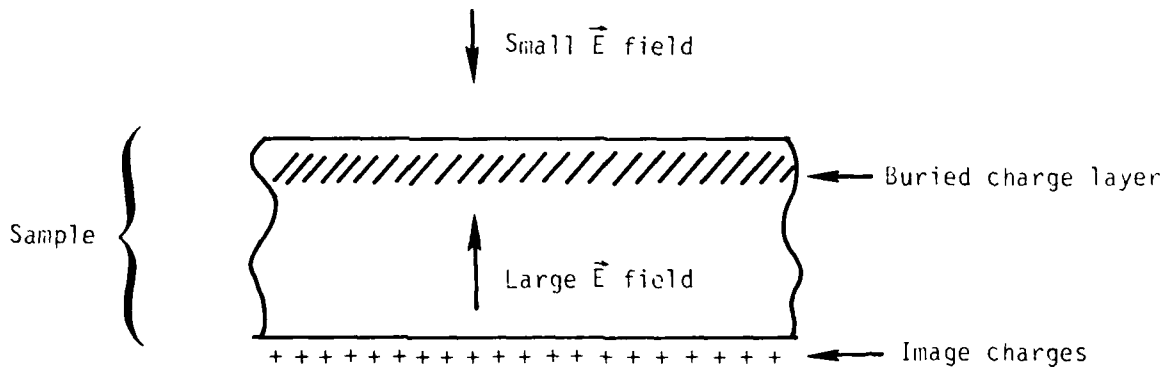
away from the surface is a function of the external field at the surface. This limitation of emission current is known as "space-charge limiting" (Fig. 12).

Clearly one would expect that the photocurrent from a dielectric would be much larger if that dielectric was charged to some large negative potential before exposure to the photons than if it was uncharged. This indeed was found to be true in all cases. Figure 13 gives an example of the emission (I_{total}) from an uncharged Teflon sample and the same sample precharged to ≈ 14 kV. Both were exposed to very similar photon pulses.

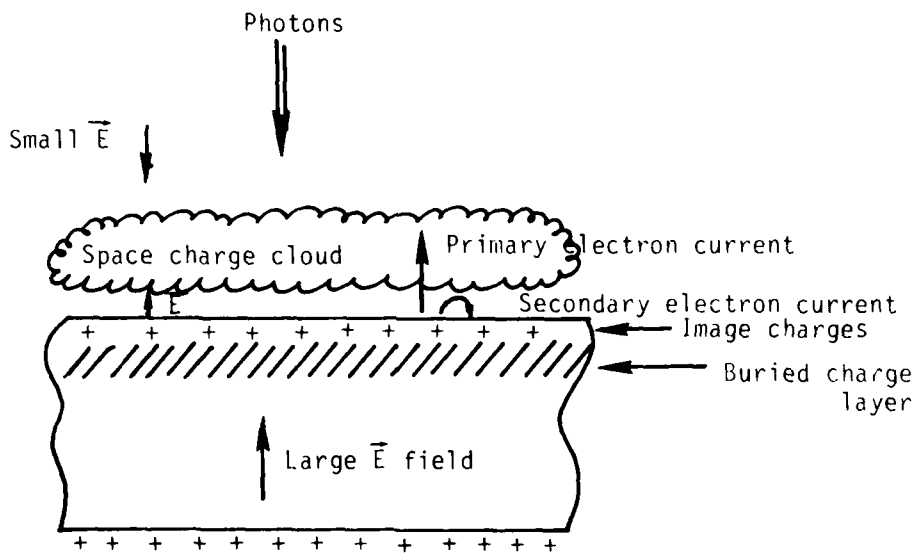
To compare these results for enhanced emission with theory, the measured instantaneous emission current density (for EWR shot #4806, 03/22/79) from a paint sample which had been precharged to 19 ± 1 kV by normally incident 30 kV electrons is shown in Figure 14. Also shown on this figure are three theoretical predictions resulting from a two-dimensional self-consistent particle-pushing code (SEMP).

For these calculations, a grid spacing of 1 cm was used, but the dielectric constant was increased ($\approx 16X$) to maintain the correct charge-to-substrate capacitance (Ref. 9). The photoelectron spectral distribution was given the form $N(E) \approx kE \exp(-E/E_0)$.

The curve marked "No Precharge" is photoemission one would expect from an uncharged paint dielectric exposed to an EWR spectrum of the same flux and time history as Shot #4806. The other two calculations were produced by a model which incorporated a close approximation of the measured potential profile, photon time history, and two photoelectron spectra. The curve labeled "High Energy" used the commonly employed approximation that only primary electrons with energies greater than a few hundred volts can escape the object while all secondaries are returned to the sample. The third curve, labeled "Low Energy", adds in the low energy ($E_1 \approx 50$ eV) or secondary electrons, which would be returned to the object by the space



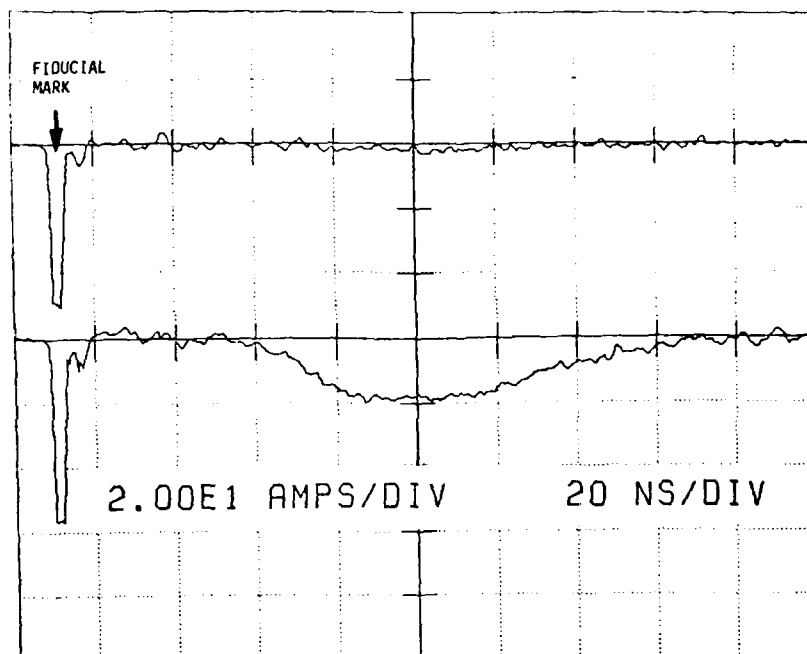
a) Before the photons



b) During photon exposure

Figure 12. Space charge limiting.

CHANNEL: 4 SHOT: 4809. DIGITIZER 4.
TEST POINT: IT0T
MAR. 22, 1979 8:58:43



CHANNEL: 1 SHOT: 4811. DIGITIZER 4.
TEST POINT: IT0T
MAR. 23, 1979 14:24:28

Figure 13. Measurements of transient current flow to and from identical points on the same teflon sample exposed to nearly equal photon bursts with the sample (a) uncharged and (b) charged to $\langle V \rangle = 11 \pm 1$ kV.

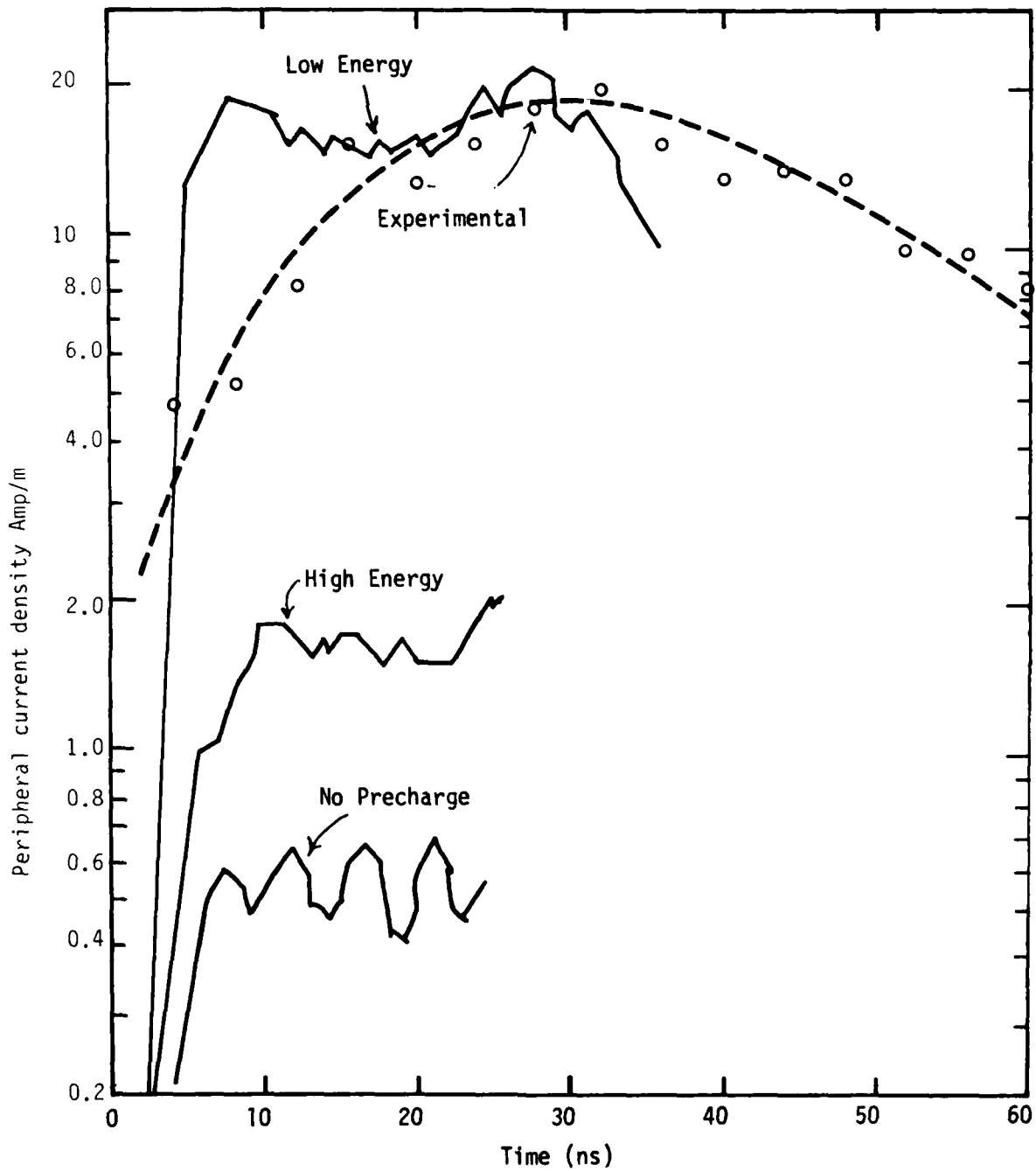


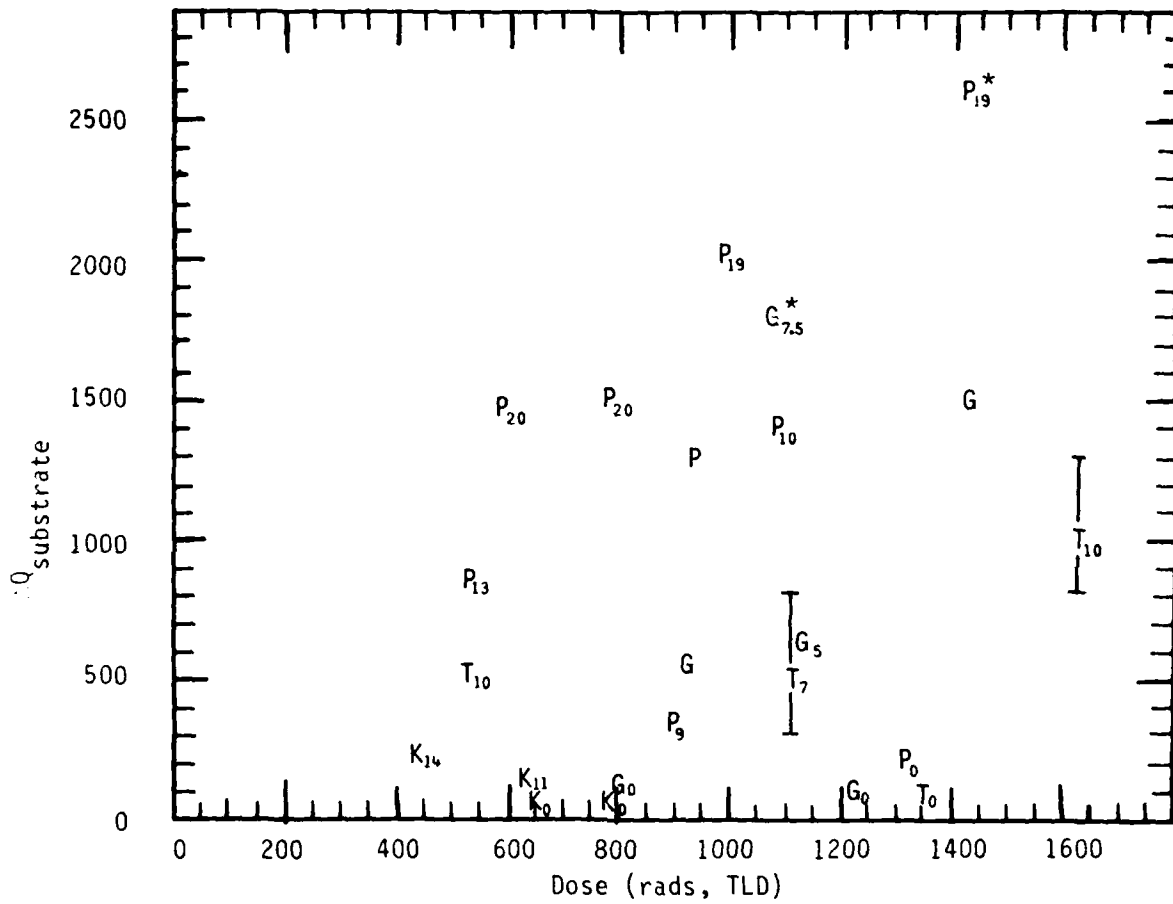
Figure 14. Comparison of measured and calculated photoemission of paint exposed to an EWR source, illustrating the significant enhancement resulting from transverse fields sweeping low energy electrons away from the precharged dielectric.

charge barrier, were the dielectric initially uncharged. The relative number of high and low energy electrons was experimentally indicated from biased diode measurements. These calculations predict a threefold emission enhancement as a result of precharging even if low energy electrons are suppressed, and a thirtyfold enhancement when low energy electrons are accounted for. The relationship between experiment and theory clearly indicates low energy electrons contribute significant current when the object has been precharged.

It should be emphasized that photocurrents of low energy electrons result from lateral charge transfer under the influence of tangential fields near the metal-dielectric boundaries. By this mechanism electrons with insufficient energy to surmount the space charge barrier are nevertheless emitted along trajectories with small normal and large tangential components. Some of these entirely escape the object, but most return to the test object or satellite, which was driven positive by the amount $\Delta V = \Delta Q/C_\infty$, where ΔQ is the charge blown off and C_∞ is the object's capacity to infinity (the tank walls). The calculations show these charges may return far from their point of origin.

According to the theory, both the charge which leaves the sample and the charge which escapes the test object should be increasing functions of both the precharge voltage and the dose of photons. Unfortunately, the data do not support this idea very well. Figure 15 shows the charge which was measured leaving the substrate plotted as a function of dose (measured with thermoluminescent detectors (TLD's) and cross-checked with x-ray diodes), with the precharge voltage given next to each data point.

There is a trend towards a dose dependence, but the trend is far from simple. We suggest that this variability is not due to uncertainties in the measurements so much as other parameters which were not documented. Culprits might include: ageing of the samples, previous spontaneous discharge history, details of the charging process like current density and



P = paint
 K = Kapton
 T = Teflon
 G = solar cell cover glass

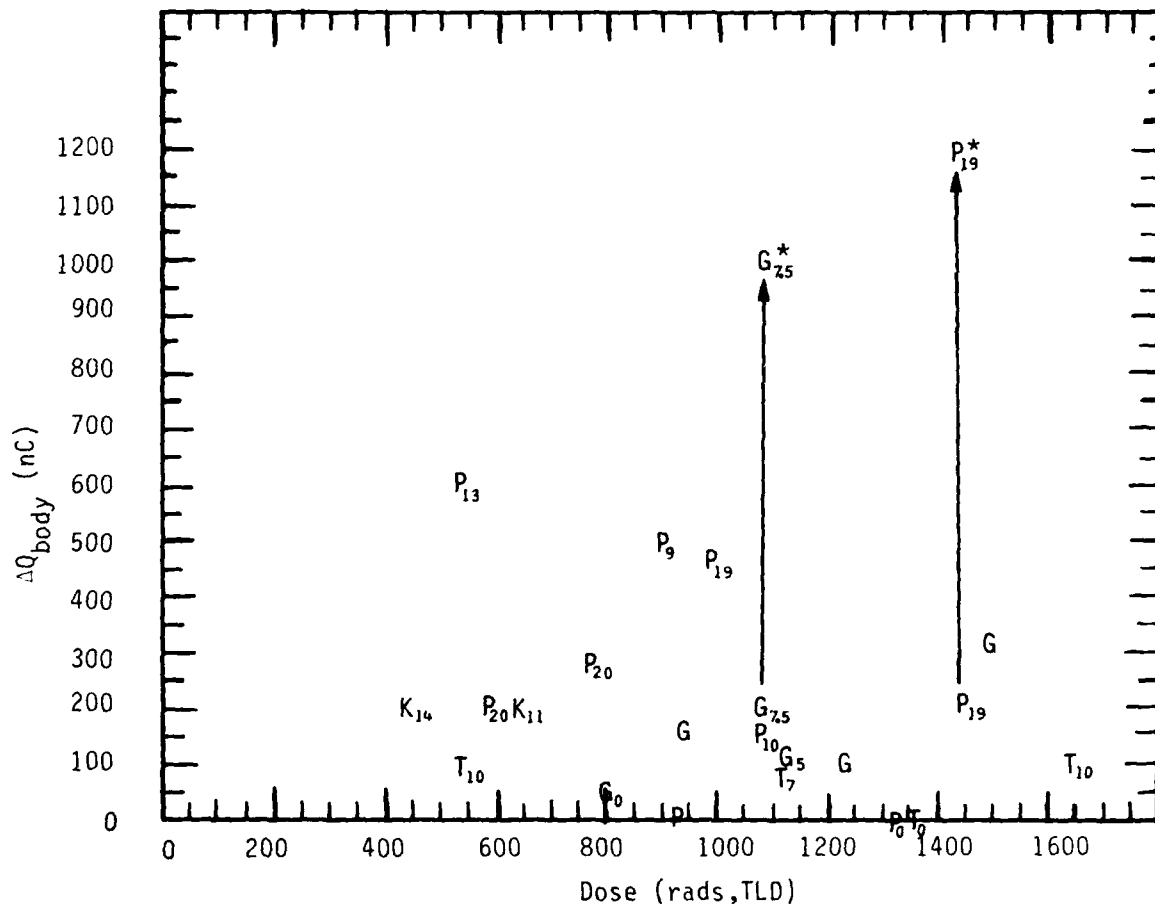
Figure 15. Charge leaving substrate vs. dose.
 (Pre-shot average voltage in kV shown
 after data point.)

energy of the beam, or build-up of contaminants on the sample surface (which was noted at least once during the test sequence). Nonetheless, it is true that the four shots on paint done while charged to 19 or 20 kV show a definite increase in emission with increasing dose. Figure 16 displays the same data the other way around - vs. voltage with dose after each data point. Here we see again a suggestion of an increasing function, but some points seem quite out of place compared with others.

Figures 17 and 18 show equivalent plots for the charge which escaped the test object vs. dose and pre-shot average voltage. Again, functional dependences are elusive. We should mention, though, that three paint shots stand out as having considerably more emission (450-600 nC) at relatively low pre-shot voltages (8-13 kV). These three shots were taken on the first day of the test sequence, nearly a month earlier than all the other paint shots. We find no evidence of any change in the experimental configuration, but it seems clear there was something different that day, possibly some difference in the preparation of the surface of the sample.

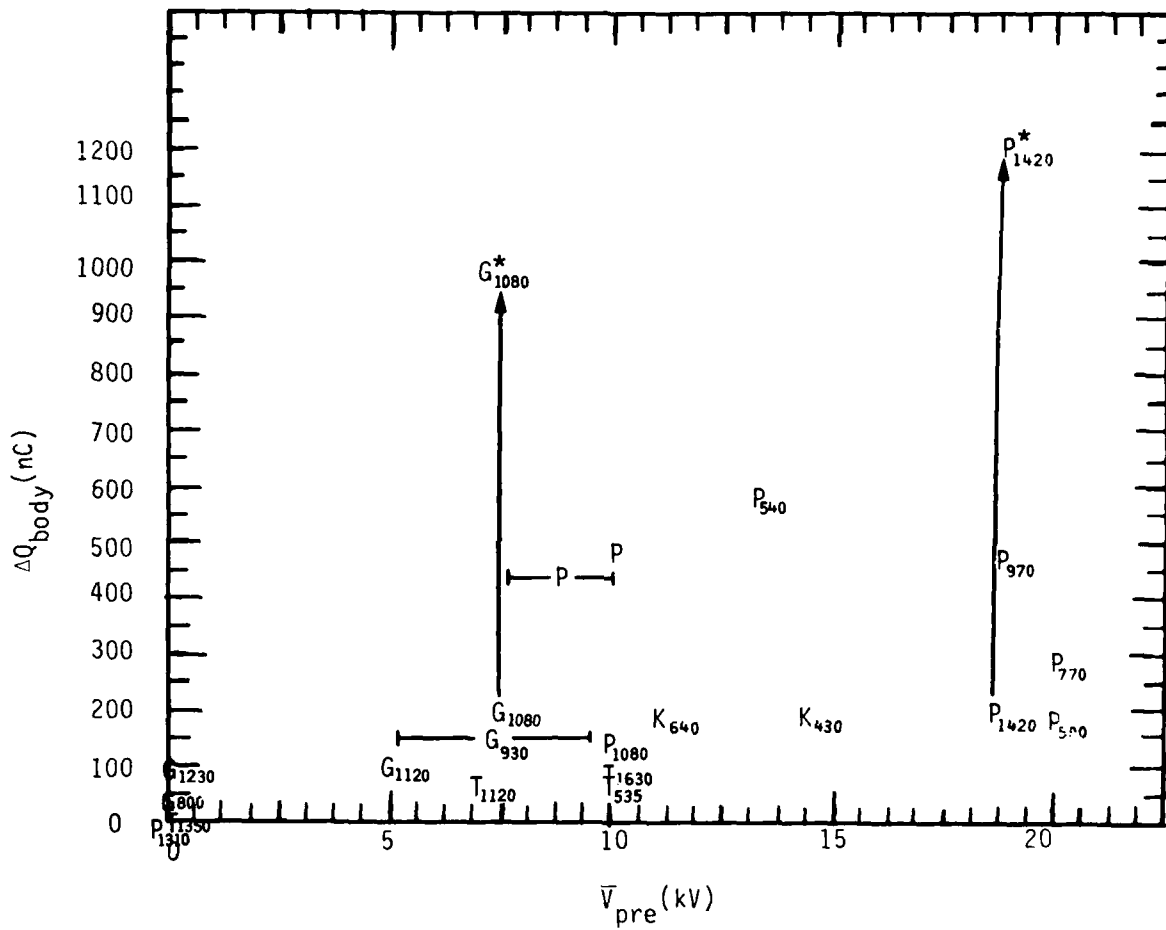
One might suppose that even though the substrate charge and the test object charge don't bear a simple relationship to voltage and dose, still they might bear a simple relationship to each other. Figure 19 shows that this is not obvious. Again we see the three paint shots stand out. Note that the 45° line indicates points for which all the charge which left the sample also left the test object.

Note on error bars on Figures 15 through 19: the error bars on the figures do not indicate the experimental uncertainties in the ordinary sense, rather they represent the range which actual measurements covered. For the charge leaving the test object, the measurement uncertainty was ± 250 V, while the capacitance was uncertain to $\pm 25\%$. The pre-shot voltage would typically vary by 2-3 kV over the area of the sample. The substrate



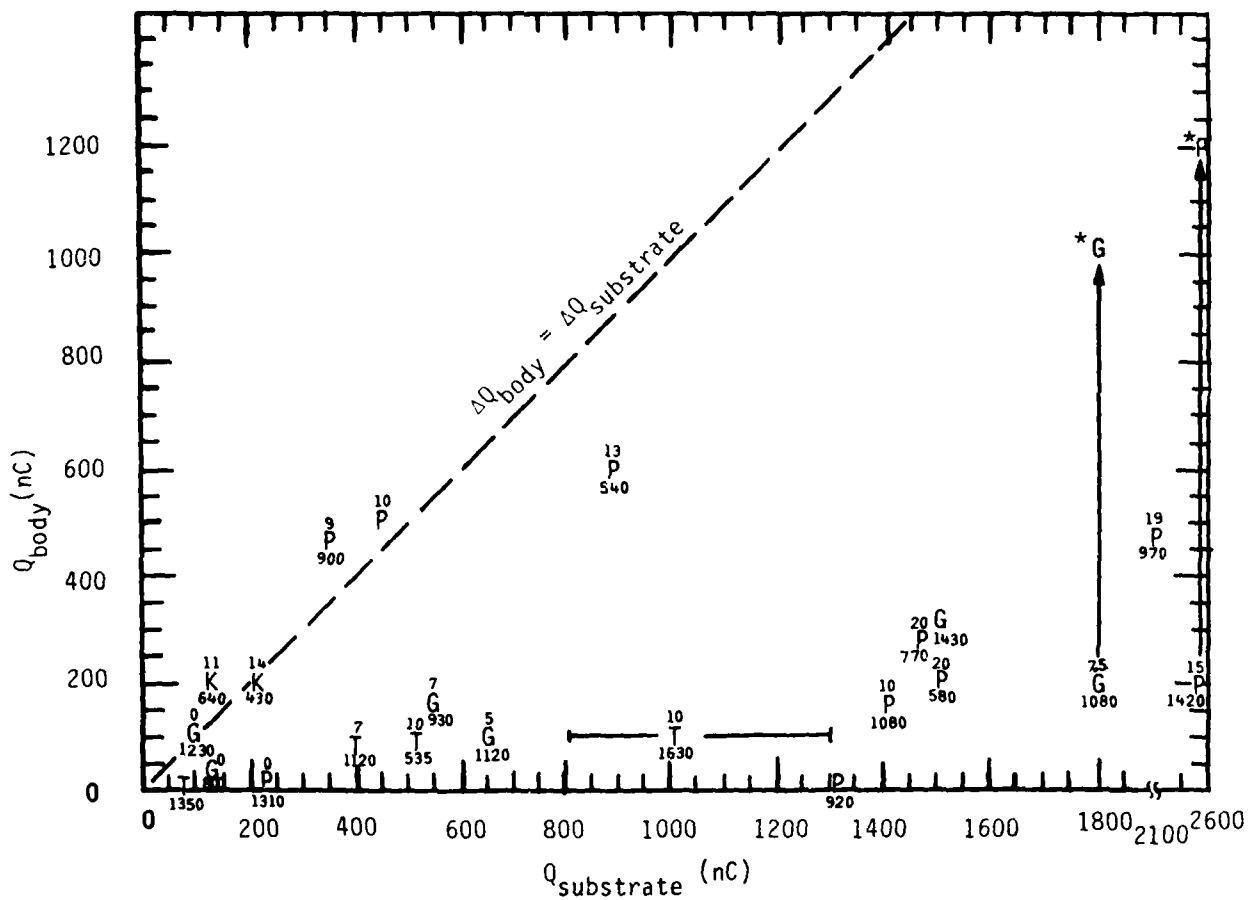
P = paint
 K = Kapton
 T = Teflon
 G = solar cell cover glass

Figure 17. Charge leaving the test object vs. dose.
 (Pre-shot average voltage in kV shown after data point.)



P = paint
 K = Kapton
 T = Teflon
 G = solar cell cover glass

Figure 18. Charge leaving test object vs. pre-charged average voltage



P = paint
 K = Kapton
 T = Teflon
 G = solar cell cover glass

Figure 19. Charge leaving test object vs. charge leaving substrate.

current measurement accuracy was limited by the non-linearities and non-reproducibility of the fiber-optic links, which is very difficult to estimate, even after calibrating. The dose measurement was provided by Physics International, from TLD measurements. While these TLD's were rated at 10% accuracy, calorimeters were used as back-up, and there were inconsistencies between these two measurements of 30%.

3.3 DELAYED SGEMP EMISSION

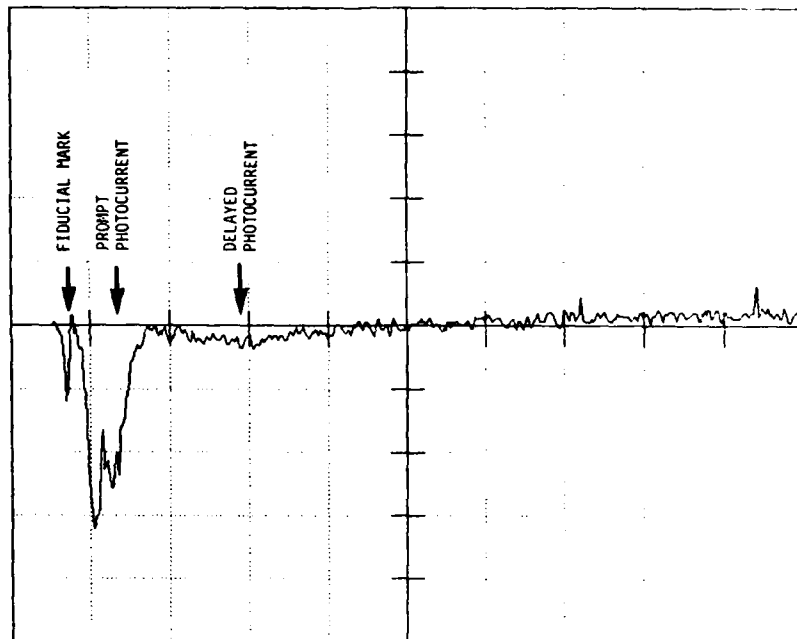
On Figures 15 through 19, there are two points which are marked with an asterisk (*). These points represent shots where there occurred a delayed emission of charge from the test object. Figures 17 and 18 show that at the end of the shot ≈ 200 nC had been emitted, then within 1 μ s, another 800-1000 nC were released.

Figure 20 shows the measured response of thermal control paint, precharged to about 19 kV. In addition to the normally observed prompt photoemission, this sample shows a component of current both in the substrate and in the body current lasting for ≈ 500 ns and delayed 100 to 200 ns from the photon pulse. This delayed current was also evidenced by the test object potential. Figure 21 compares the body potential for two consecutive nearly identical exposures. No delayed emission was observed for the former (Shot #4806). The test body potential increased in less than 100 ns to approximately 1 kV and decayed at the 10 μ s RC time constant. The body potential for Shot #4807 also rapidly increased to approximately 1.5 kV, but then continued to increase during the emission of the delayed component. This implies that an additional 0.96 μ C was emitted and that it did not return to the body.

The characteristics of these two events were quite different than the events observed by van Lint, et al., (Ref. 1), which was much larger, faster and earlier, relative to the prompt signal. Nonetheless we cannot

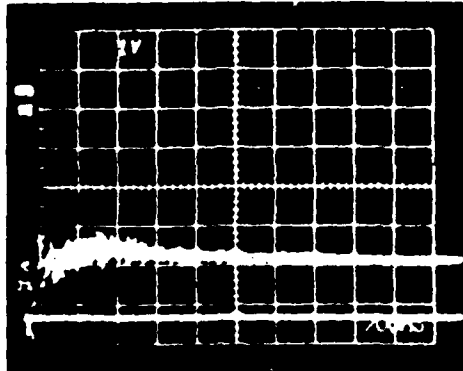
1.00E0 AMPS/DIV

200 NS/DIV

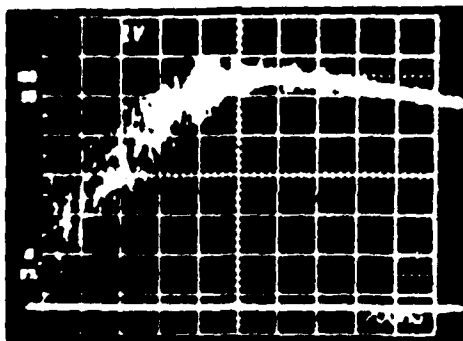


CHANNEL: 4 SHOT: 4807. DIGITIZER 2.
TEST POINT: 15
MAR. 22, 1979 14:49:28

Figure 20. Transient current record showing the prompt and delayed current component.



(a) Shot #4806 with ≈ 100 ns photoemission.



(b) Shot #4807 which displayed delayed emission.

Figure 21. Test object voltage (10^3 V/div) versus time (200 ns/div). Shots 4806 and 4807.

rule out the possibility that these events represent another manifestation of the infamous "triggered discharge". We observe that these events happened following a large dose (though not the largest) when the sample was charged to nearly the highest voltage.

SECTION 4 SUMMARY

1. Surface potentials in excess of 15 kV can be sustained by Kapton, Teflon, paint, and fiberglass; with gradients of 10^6 V/m (at edges). Considerable fine-scale structure was noted. Observed potential decay rates are consistent with typical dielectric resistivities of 10^{16} to 10^{18} ohm cm. Spontaneous discharges and photo-induced charge transfers on the order of 2 μC were common, as compared to blow-off transfers of approximately 0.2 μC . Numerous examples of radiation-induced charge redistribution were noted.
2. Enhanced prompt SGEMP response was noted for all samples. These emissions approximately followed the time history of the photon pulse, but with an amplitude 5 to 20 times larger than the uncharged sample. This observation is quantitatively explained and is attributed to the lateral transfer of low energy electrons under the influence of previously existing fields.
3. Contrary to the Skynet Qualification Model observations, no "triggered discharges" were observed in this series. However, on two occasions the paint sample exhibited an anomalous delayed component of current lasting ≈ 500 ns. This was noted in both the substrate-to-body current and between the sample and vacuum chamber implying net charge loss from the body rather than just charge transfer on the object.

4. Solar cells, regardless of size (2×2 or 4×4 cm) or thickness (0.006 or 0.012 in) spontaneously discharged at approximately 9 ± 1 kV (e-gun voltages of 11 to 12 kV). These discharges showed considerable variation in nature and magnitude from less than 1 μC to much more than 10 μC .
5. Measurements of charge profiles on solar panel structures demonstrated that the potential above fiberglass around the edges typically exceeds the coverglass potential by approximately 60 percent. A qualitative explanation of the previously observed triggered discharge is that it results from photo-induced charge flow from the fiberglass to the coverslip, followed by a process indistinguishable from spontaneous discharge.

REFERENCES

1. V.A.J. van Lint, et al., "Spontaneous Discharges and the Effects of Electron Charging on Skynet SGEMP Response," IEEE Trans. Nucl. Sci., NS-25, 1293 (1978).
2. V.A.J. van Lint, B.C. Passenheim, R. Stettner, D.A. Fromme, "The Effect of Electron Precharging on SGEMP Response of Insulators," IEEE Trans. on Nucl. Sci., NS-26, No. 6, (1979).
3. J.D. Riddell, V.A.J. van Lint, and B.C. Passenheim, "Charging and Discharging of Satellite Dielectrics," Mission Research Corporation, MRC/SD-R-70, Jan 1981.
4. M.J. Bernstein, "Photoelectron Energy Spectra Generated by Low Energy X-Ray from Intense Plasmas," IEEE Trans. Nucl. Sci., NS-24, 2512 (1977).
5. D.A. Fromme, et al., "Electron Emission Spectra Produced by Exploding Wire Photon Sources," IEEE Trans. Nucl. Sci., NS-24, 2429 (1977).
6. D.A. Fromme, et al., "SGEMP Response Investigation with Exploding Wire Photons," IEEE Trans. Nucl. Sci., NS-24, 2371 (1977).
7. D.A. Fromme, et al., "Exploding Wire Photon Testing of Skynet Satellite," IEEE Trans. Nucl. Sci., NS-25, 1359 (1978).
8. M.L. Price, et al., "Electrical and Photon Tests of a Resonant Satellite Shape," IEEE Trans. Nucl. Sci., NS-25, 1358 (1978).
9. V.A.J. van Lint, et al., "Skynet Satellite Electron Precharging Experiments," Proceedings of the Spacecraft Charging Technology Conference at the USAFA, November, 1978; NASA Conf. Publication 2071, AFGL-TR-79-0082.
10. V.A.J. van Lint, B.C. Passenheim, "Charging and Discharging of Teflon", Proceedings of the Spacecraft Charging Technology Conference, 1980, NASA Conf. Pub. 2182, AFGL-TR-81-0270.

APPENDIX

THE EFFECT OF ELECTRON PRECHARGING ON SGEMP RESPONSE OF INSULATORS*

V. A. J. van Lint, B. C. Passenheim, R. Stettner, D. A. Fromme**

Mission Research Corporation
P. O. Box 1209
La Jolla, California 92038

1. Introduction

The effects of low energy (5 to 30 keV) electron precharging on the SGEMP response of several common satellite materials exposed to photons from an exploding wire radiator (EWR) are reported here. The EWR source produces a narrow (50-100 ns) fast risetime (~ 10 ns) low photon energy ($E \sim 2$ keV) pulse which results in low energy photoelectron emission.^{1,2} This EWR source has been used for previous SGEMP experiments on simple objects,³ on a structural model of the Skynet satellite⁴ and on a simple model of a resonant structure.⁵ EWR exposures of an electron precharged Skynet Qualification Model satellite⁶ established that the SGEMP response was enhanced by precharging either the thermal paint or solar cell covers, and that on one occasion, a massive discharge of solar cell covers appeared to be triggered by the EWR exposure.

The present experiment was designed to study SGEMP enhancement and discharge triggering under controlled and measured conditions to provide data for comparison with theoretical calculations to identify the causal parameters.

In Section 2 we describe the experiment in sufficient detail to establish experimental uncertainties and lend credence to our inferences. In Section 3 we present selected examples of experimental observations. Section 4 is a summary of the results.

2. Experimental Details

The exterior geometry of the test structure is indicated in Figure 1. In all cases the dielectric samples were 82 cm in diameter supported on an 85 cm diameter, 0.95 cm (3/8") thick plexiglass disk. The samples were mounted on the front of a 120 cm diameter by 51 cm long aluminum cylinder. The dielectric materials investigated were:

- (1) Back-surface aluminized kapton, 82 cm (32 in) in diameter, 0.013 cm (0.005 in) thick stretched over the plexiglass disk.
- (2) Back-surface silvered teflon, 82 cm in diameter, and 0.013 cm thick stretched over the plexiglass disk.
- (3) Silicon alkyde white thermal control paint approximately 0.013 cm thick applied to an 85 cm diameter fiberglass disk approximately 0.035 cm (0.014 in) thick on a segmented copper back plate. The segmented copper plate had a 27 cm diameter central disk surrounded by segmented rings (shown dotted in Figure 1). This multilayer structure was cemented to the plexiglass disk.
- (4) A 50 cm x 50 cm array of 0.030 cm (0.012 in) thick MgF₂ coated fused silica solar cell cover slips. These slips covered copper tape configured to electromagnetically simulate cells, on a 0.035 cm thick fiberglass sheet supported on the plexiglass disk. The array was composed of both 2 cm x 2 cm and 4 cm x 4 cm cells. The spacing between the cells (~ 0.050 cm), conductor

*Work performed under Defense Nuclear Agency Contracts DNA001-77-C-0009 and DNA001-78-C-0269.

** Mr. Fromme is now at Lawrence Livermore Laboratories, Livermore, California.

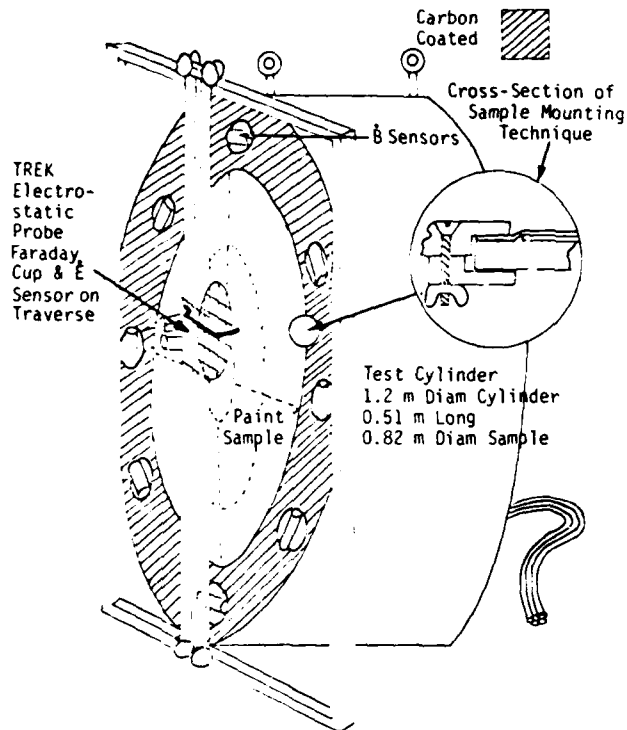


Figure 1. Picture of the test body showing traverse, sample and B sensors. Insert shows the way the sample was attached to the test body.

routing, and the interconnections of the copper tape were designed to mimic actual solar panel geometry as closely as possible.

For comparison purposes, the range of a 30 keV electron is about 20 μ m in plastic, the absorption depth of a 1 keV photon is 5 μ m and that of a 2 keV photon is 30 μ m. The samples were all at least 125 μ m thick.

Interconnect tabs on real solar cells are flat strips bent into the shape of an omega (Ω), to provide strain relief, which causes a conducting hairpin to extend above the surface of the cell cover. This physically small feature might appreciably alter the discharge characteristics of solar cell cover arrays, as it introduces a conductor in the plane of the surface charge. These interconnects were simulated over approximately ten percent of the array with short pieces ($\sim 1/8$ in) of 0.050 cm (0.020 in) diameter wire soldered to the copper tape between adjacent cell covers. Other areas of the array were without simulated interconnect protrusions. (No difference was noted.) Cell covers and copper tape were intentionally deleted from a few portions of the array, (1) to simulate areas near penetrations, and (2) to provide a sufficient area to reliably measure fiberglass surface potential with an electrostatic voltmeter.

The dielectric samples were surrounded by eight EG&G CMLX3B B or surface current sensors oriented to

detect radial current flow (schematically indicated in Figure 1).

The magnitude and time history of spontaneous discharges and SGEMP emissions were measured with EG&G β surface current probes, or by measuring currents from the cylinder to the conducting substrates of the samples with Tektronix CT-2 current transformers. In the cover glass array and thermal control paint samples, information about charge redistribution within the dielectric (as opposed to blow-off or punch-through) was inferred from currents flowing between the segmented metal substrates. These currents were also measured with current transformers.

Fast transient data was transmitted to the recording instrumentation through HDL/DNA 400 MHz fiber optic data links recorded on Tektronix 7912 transient digitizers and processed on a PDP/1140 computer.

The test cylinder was connected to instrumentation ground through a 50 k Ω resistor chain. This provided cylinder potentials of less than 0.5 V during charge at measured densities of $\sim 10^{-9}$ A/cm². However, the RC time constant of this resistor string and cylinder capacitance to the tank (~ 240 pf) was calculated to be about 10 μ s, so the test structure was effectively isolated during spontaneous discharges and EWR photon pulses which are generally less than 0.1 μ s (FWHM).

As shown in Figure 1, the front of the cylindrical test object was surrounded by a square frame which supported small motors, pulleys, and belts (not shown) to drive a traverse carrying the probe of a TRECK non-contacting electrostatic voltmeter, a Faraday cup, and an E sensor over the surface of the sample. The spatial resolution of the electrostatic voltmeter is estimated to be ± 3 mm, the Faraday cup area was approximately 1 cm², and the E probe was used as an oscilloscope trigger in spontaneous discharge studies. Both the traverse frame and aluminum ring surrounding the dielectrics were coated with colloidal graphite, to (1) inhibit dielectric charging, and (2) minimize photoelectron emission from the aluminum.

An expanded inset in Figure 1 indicates how the samples were held in the cylinder. The 3/8 in thick plastic support disks were inserted through the removable aluminum back of the test cylinder and clamped in a ring cut in the back of the front face. Thus, the truly flat samples (Teflon and Kapton) were recessed 0.25 cm (0.100 in) below the front aluminum ring. The edge of the aluminum ring touching the dielectric had been machined and finished using typical machine shop practice. The edge of this ring had been "broken," that is, the sharp edges from the cutting operation had been softened with a fine file or sandpaper to produce a corner with a radius of curvature on the order of 0.025 to 0.050 cm (0.010 to 0.020 in).

Figure 2 is a representation of the experiment's overall test geometry. The test cylinder was suspended very nearly in the center of the 10 ft diameter, 12 ft long vacuum tank. Since the object hung on the nylon ropes from a rotary feedthrough, it could be rotated about a vertical axis passing through the cylinder center, along a diameter "in situ" to point in any direction. Non-normal orientations permitted investigations of the effect on the surface potentials of charging at non-normal angles. Photon time histories and shot-to-shot fluence variations were monitored with four (300V) biased fast diodes previously discussed in Reference 2. These 50 Ω diodes were mounted near the back wall of the chamber and were hardwired to 7904 scopes with copper-jacketed 50 Ω coaxial cable. Two diodes were gold, one was glass, and one was paint. The photoelectron emission of gold exposed to the EWR source has been studied by MRC and others

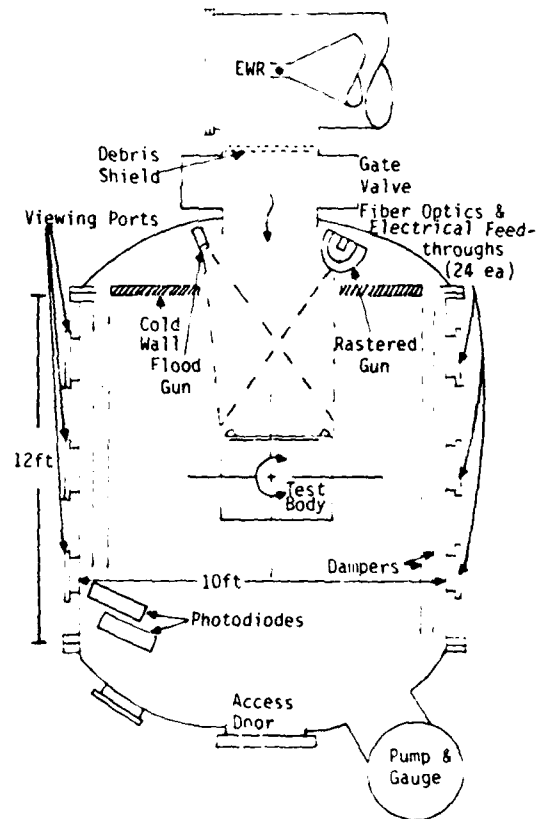


Figure 2. Top view of the SGEMP/SCC experiment chamber.

(Reference 1). The glass and paint photodiodes served to define the photoelectron emission relative to gold. Because these diodes were located in the periphery of the electron gun emission pattern, it is not likely that they reached the same surface potential as the test material except in cases where the sample was charged for extended periods. Nevertheless, enhanced emission from precharged dielectrics was clearly observed.

The tank was lined with two cylindrical layers of ~ 200 ohm/sq carbon-coated sail cloth damper to suppress tank wall photoemission and damp tank EM resonances. The dampers were nominally located at 80 and 90 percent of the tank diameter, and were open at each end.

During the course of the experiment, two 0-30 kV electron guns were employed. These guns were located symmetrically on either side of the EWR port. One was a flood gun, previously described in Reference 3, constructed for DNA by IRT Corporation. Faraday cup measurements indicated that this gun provided illumination which differed by less than a factor of two from the center to the edge of the sample. Acceleration potential was determined by floating the gun filament supply to a negative potential with respect to a fine wire grid with a controlled high voltage supply. Gun current was regulated with a feedback circuit which sensed gun emission current and modulated the filament supply power. The other (rastered) gun was constructed by MRC/SD and was designed to illuminate the sample with a small diameter (~ 2 cm diameter) spot. This gun was constructed from an electrostatically focused and deflected cathode ray tube gun. Potential and current were controlled as with the flood gun. Acceleration was achieved by controlling the bias between two hemispherical baskets surrounding

the gun and concentric with the final deflection plates. For equal total beam currents, the current density in the beam of the rastered gun was ~ 1600 times greater than from the flood gun. A limited comparison on each of the four sample types did not indicate any startling disparities in the ratio of surface potential to gun acceleration voltage. That is, there were no obvious rate effects. A liquid nitrogen-cooled annular copper ring surrounded the exposure port. A 1 meter diameter gate valve separated the EWR source chamber from the test chamber between shots, when the source chamber was vented to change wires. A 70 percent transmitting copper screen and 0.005 inch mylar debris shield protected the test chamber vacuum from the pressure pulse in the source chamber which accompanies the photon pulse.

The pressure in the test chamber was typically $4.0 \pm 0.5 \times 10^{-6}$ torr prior to a shot. From numerous measurements, we determined that after charging the dielectric to 10 to 16 kV, the sample potential decayed at a rate of 20 to 70 V/min at pressures below 1×10^{-4} . Assuming the principal charge loss mechanism was conductivity through the sample as opposed to air ionization, one would infer bulk resistivities of 10^{17} to 10^{18} ohm cm for kapton and teflon, and 10^{16} to 10^{17} for paint and cover glasses. These values are consistent with the range of values offered in material properties handbooks. Several times we intentionally increased the pressure in the test chamber by closing the gate valves and warming the cold wall, and found that the decay rate was apparently insensitive to pressure below 2×10^{-4} and was erratic but rapid (about 10^3 V/s) at greater pressures. From Paschen's gas discharge curve, one would expect rapid discharge of surfaces charged to $\sim 10^4$ V and separated by more than 10 cm at approximately 2×10^{-4} torr.

The test chamber was continuously monitored. Occasionally, the debris shield was ruptured or punctured at shot time and the chamber pressure would rise to $\sim 3 \times 10^{-4}$ torr. On shots where the debris shield retained integrity, the pressure never exceeded 3×10^{-5} torr. A comparison of the pre-to-post shot potential (charge) profile was considered valid only when the pressure remained below 1×10^{-4} torr. However, even when the debris shield was compromised, and the pressure ultimately exceeded 10^{-4} torr, the fast transient data is still valid since the measurements were completed (~ 100 ns) long before the sample was exposed to the pressure surge (~ 1 ms).

3. Experimental Results

3.1 Potential Profiles and Charge Transfer

Figures 3(a) and 3(b) show the measured potential (charge) profile on the paint sample before and after OWL II shot #4805 executed at 11:37 on 03/22/79. The average potential profile before the shot is 13 ± 1 kV with peak potentials of 16 kV. The average potential after the shot is 10 ± 1 kV with peak potentials of 13 kV. This sample had been charged with 25 kV electrons at nearly normal incidence. Notice that the potential (charge) profile has considerable structure. Although this short range structure is characteristic of the sample rather than the source and was observed for all sample types, it is only partially reproduced on successive charging. This pre-shot profile was taken 55 ± 5 minutes before the shot. The post-shot profile was taken between 5 and 10 minutes after the shot. For 30 minutes immediately after the pre-shot profile measurements, the potential at one selected point was monitored. From this measurement, we found the potential leaked away at a rate of 55 ± 5 V/m.

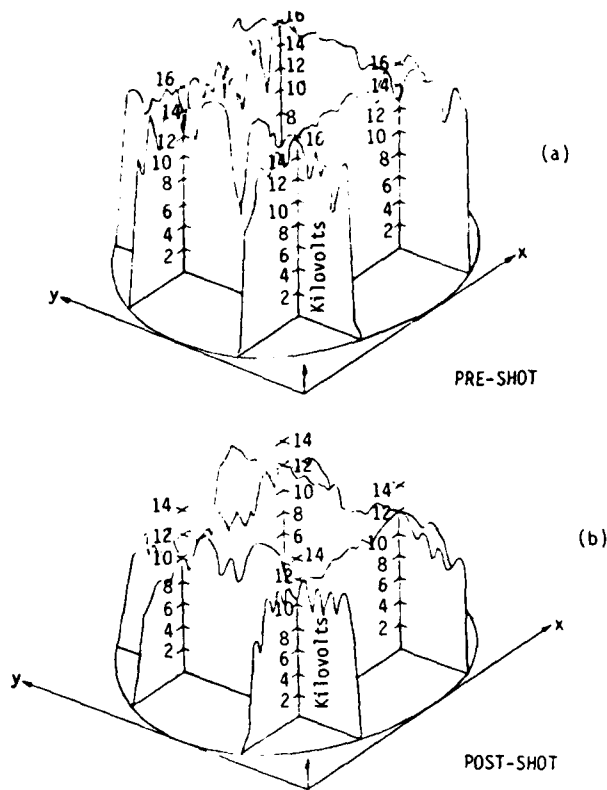


Figure 3. Potential profile of a sample of thermal control paint precharged with 25 keV electrons at near normal incidence, before and after EWR exposure.

The measured capacitance from the sample surface to the metal backplate is approximately 20 nF. The pre- and post-shot voltage profiles indicate a net charge loss from $\Delta Q = C \Delta V$ of $2 \times 10^{-8} \times 3 \times 10^3 = 60 \mu\text{C}$, which is almost entirely accounted for by the static charge loss $\Delta Q = C \frac{dV}{dt} \Delta t = 20 \text{ nF} \times 55 \text{ V/min} \times 55 \text{ min} \approx 60 \mu\text{C}$. Successive traverses over the same area show that the potential sags uniformly. This is what one would expect, since except for a band approximately 1 mm thick around the periphery of the sample, the field is primarily directly across the thin dielectric. Under these circumstances, the potential loss rate implies dielectric (paint and fiberglass resistivity) of $\rho = VA/Cd(\Delta V/\Delta t) \approx 5 \times 10^{16}$ ohm cm. Figure 4 is a composite of the measured transient currents to the backplate during the shot. The integral of these currents is

$$\Delta Q \int_0^{\infty} I(t) dt \approx 2 \mu\text{C}.$$

Furthermore, these measured currents include both the charge that flows from the dielectric to the metal test object as well as the charge blown off to infinity. One can infer the fraction of charge blown off from the potential obtained by the test object. In this particular case, the test object rose to approximately 1 kV, which implies that only $Q = C \Delta V \approx 0.24 \mu\text{C}$ actually escaped the test object.

Finally, notice that the potential minimum noted prior to the exposure [see Figure 3(a)] is definitely absent after the EWR exposure. This is one of numerous

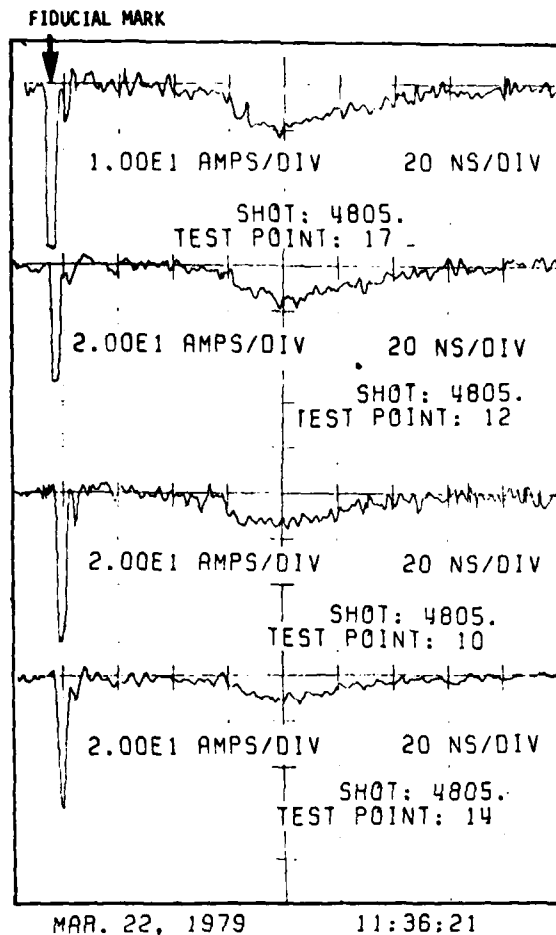
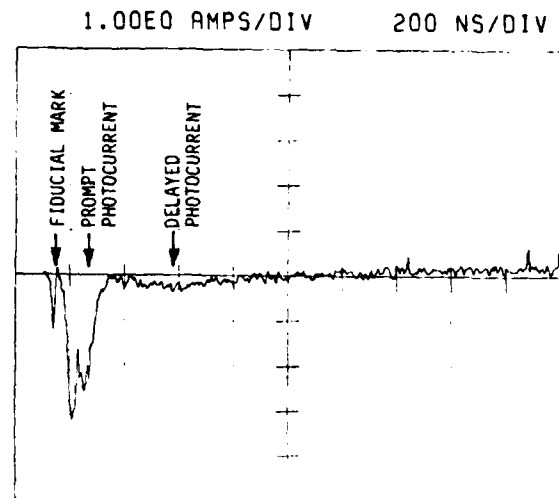


Figure 4. Transient current flow from the test body to the metal backing of the fiberglass sample during EWR exposure.

examples of charge redistribution. In this particular case, a charge transfer of $\sim 1.6 \mu\text{C}$ is required to change the potential of a 10 cm wide valley by $\sim 4 \text{ kV}$.

3.2 Delayed SGEMP Emission

Although no "triggered discharge" (where the term "triggered discharge" describes a massive charge transfer initiated approximately 100 ns after the arrival of the photon burst) was noted in this test series, on two occasions the paint sample exhibited delayed photocurrent. Figure 5 shows the measured response of thermal control paint, precharged to about 15 kV. In addition to the normally observed prompt photoemission, this sample shows a component of current both in the substrate and in the body current lasting for $\sim 500 \text{ ns}$ and delayed 100 to 200 ns from the photon pulse. This delayed current was also evidenced by the test object potential. Figure 6 compares the body potential for two consecutive nearly identical exposures. No delayed emission was observed for the former (Shot# 4806). The test body potential increased in less than 100 ns to approximately 1 kV and decayed at the 10 μs RC time constant. The body potential for Shot# 4807 also rapidly increased to approximately 1.5 kV, but then continues to increase during the emission of the delayed component. This implies that an additional 0.96 μC was emitted and that it did not return to the body.



CHANNEL: 4 SHOT: 4807. DIGITIZER 2.
TEST POINT: 15
MAR. 22, 1979 14:49:28

Figure 5. Transient current record showing the prompt and delayed current component.

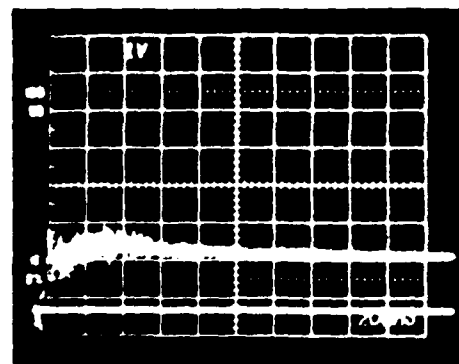


Figure 6(a). Test object voltage (10^3 V/div) versus time (200 ns/div), Shot# 4806 with $\sim 100 \text{ ns}$ photoemission.

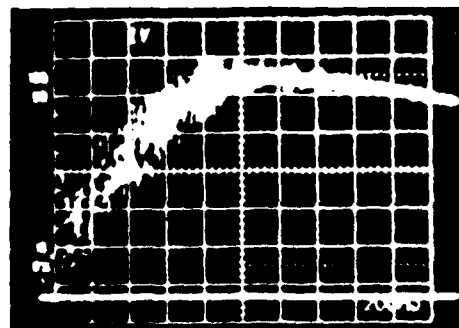
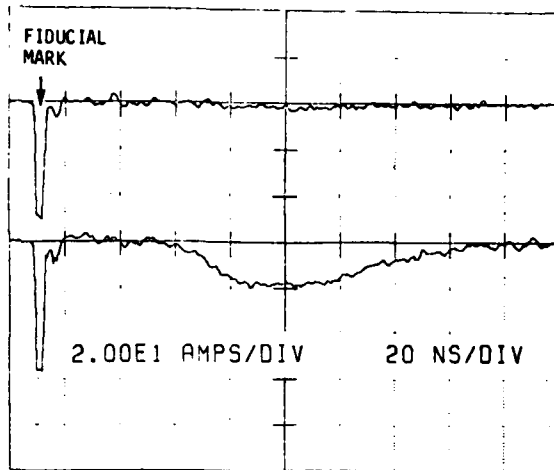


Figure 6(b). Test object voltage (10^3 V/div) versus time (200 ns/div), Shot# 4807 which displayed delayed emission.

3.3 Enhanced SGEMP

Figure 7 compares the charged and uncharged transient photocurrent emission from silver-backed teflon

CHANNEL: 4 SHOT: 4809. DIGITIZER 4.
TEST POINT: 1T0T
MAR. 22, 1979 0:58:43



CHANNEL: 1 SHOT: 4811. DIGITIZER 4.
TEST POINT: 1T0T
MAR. 23, 1979 14:24:28

Figure 7. Measurements of transient current flow to and from identical points on the same teflon sample exposed to nearly equal photon bursts with the sample a) charged, and b) charged to $\langle V \rangle = 11 \pm 1$ kV.

exposed to OML II/EWR Shots# 4809 and 4811. As with all the dielectrics studied in this series, a substantial (10X) increase in emission is noted as a result of precharging.

3.4 Comparison With Theory

The measured instantaneous emission current density (for EWR Shot# 4806, 03/22/79) from a paint sample which had been precharged to 15.3 ± 1 kV by normally incident 30 kV electrons is shown in Figure 8. Also shown on this figure are three theoretical predictions resulting from a two-dimensional self-consistent particle-pushing code (SEMP).

For these calculations, a grid spacing of 1 cm was used, but the dielectric constant was increased ($\sim 16X$) to maintain the correct charge-to-substrate capacitance (Reference 7). The photoelectron spectral distribution was given the form $N(E) \sim kE \exp(-E/E_0)$.

The curve marked "No Precharge" is photoemission one would expect from an uncharged paint dielectric exposed to an EWR spectrum of the same flux and time history as Shot# 4806. The other two calculations were produced by a model which incorporated a close approximation of the measured potential profile, photon time history, and two photoelectron spectra. The curve labeled "High Energy" used the commonly employed approximation that only primary electrons with energies greater than a few hundred volts can escape the object while all secondaries are returned to the sample. The third curve, labeled "Low Energy" incorporates low energy ($E_1 \sim 50$ eV) or secondary electrons, which would be returned to the object by the space charge barrier, were the dielectric initially uncharged. The relative number of high and low energy electrons was experimentally indicated from biased diode measurements. These calculations predict

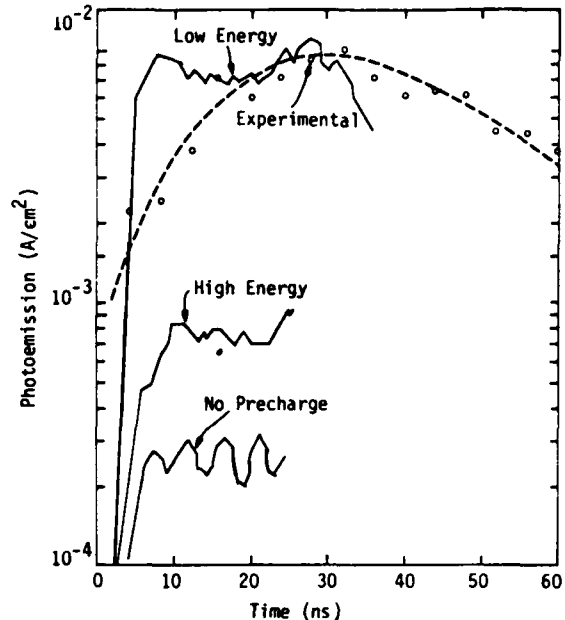


Figure 8. Comparison of measured and calculated photoemission of paint exposed to an EWR source, illustrating the significant enhancement resulting from transverse fields sweeping low energy electrons away from the precharged dielectric.

a threefold emission enhancement as a result of precharging if low energy electrons are suppressed, and a thirtyfold enhancement when low energy electrons are accounted for. The relationship between experiment and theory clearly indicates low energy electrons are critical when the object has been precharged.

It should be emphasized that photocurrents by low energy electrons result from lateral charge transfer under the influence of tangential fields near the metal dielectric boundaries. By this mechanism electrons with insufficient energy to surmount the space charge barrier are nevertheless emitted along trajectories with small normal and large tangential components. Some of these entirely escape the object, but most return to the test object or satellite, which was driven positive by the amount $\Delta V = \Delta Q/C_\infty$, where ΔQ is the charge blown off and C_∞ is the object's capacity to infinity. The calculations show these charges may return far from their point of origin.

3.5 Solar Cell Coverslips

Figure 9 shows one of many measured potential (charge) profiles along a precharged solar cell cover glass array. The principal point to note is that the coverglass potentials seldom exceed 8-10 kV, because spontaneous discharge occurs at about 9 kV. Fiberglass, on the other hand, can attain potentials in excess of 13 kV. Although we did not obtain a "triggered" discharge in this experiment series, this measured potential profile together with the previous observation that substantial lateral charge transfer is predicted and observed, suggests the following explanation.

In the previous test on the Skynet Qualification Model, electron precharging produced a potential profile with several gradients. Solar cells remained at or near ground potential, cover glass surfaces climbed to 8-10 kV before they spontaneously discharged; but fiberglass

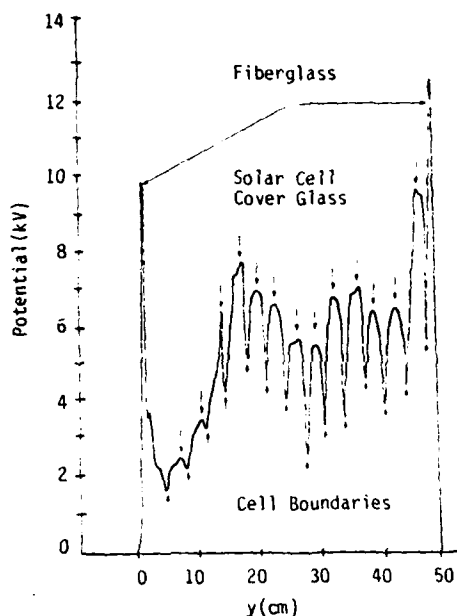


Figure 9. Potential profile along a row of charged solar cell cover glasses measured with a non-contacting electrostatic potential probe.

or thermal control paint in the vicinity of the solar cell cover glasses may have reached potentials in excess of 16 kV. The surface potential of the Qual Model was not measured because the object was geometrically complex. When the EWR burst occurred, charge was emitted from all exposed surfaces. Some charge was driven to infinity, some charge was collected by nearby low potential conducting surfaces, and some charge was transferred from the local high potential ($V > 13$ kV) fiberglass to the comparatively low potential ($V \sim 9$ kV) coverslip. The exposed interconnects in a solar cell array are miniscule (10^{-2} cm²) compared to the exposed area of the glass surfaces (4 to 16 cm²). From measurements previously described, we know photocurrents of $\sim 10^{-2}$ A/cm² were emitted by EWR exposure, and only 10 to 20 percent actually escaped the body, the remainder returning to the object. Consequently, it is reasonable to hypothesize that a significant fraction of the charge emitted from the precharged dielectric surrounding and interspersed with the cover glass was collected on the glass. During the event, while the cover glasses and substrates were immersed in a sea of free charge, the potential gradients were insufficient to cause spontaneous discharge. However, as the sea of free charge dissipated, the coverslips found themselves charged to potentials greater than that required for spontaneous discharge. Enhanced emission from a precharged object set up conditions which cannot be induced by precharging alone. Such a hypothesis provides a feasible explanation for the singular but well documented triggered discharge observed in the Skynet tests. It suggested that the failure to reproduce this effect in the most recent test series may be due to having an incorrect mix of high and low potential dielectrics, and furthermore suggests that the potentially serious triggered discharges might be controlled by minimizing the amount and/or proximity of high potential dielectrics in the vicinity of the solar array.

4. Summary

1. Surface potentials in excess of 15 kV can be sustained by kapton, teflon, paint, and fiberglass; with

gradients of 10^6 V/m (at edges). Considerable fine-scale structure was noted. Observed potential decay rates are consistent with typical dielectric resistivities of 10^{16} to 10^{18} ohm cm. Spontaneous discharges and photo-induced charge transfers on the order of 2 μ C were common, as compared to blow-off transfers of approximately 0.2 μ C. Numerous examples of radiation-induced charge redistribution were noted.

2. Enhanced prompt SGEMP response was noted for all samples. These emissions approximately followed the time history of the photon pulse, but with an amplitude 5 to 20 times larger than the uncharged sample. This observation is quantitatively explained and is attributed to the lateral transfer of low energy electrons under the influence of previously existing fields.

3. Contrary to the Skynet Qualification Model observation, no "triggered discharges" were observed in this series. However, on two occasions the paint sample exhibited a delayed component of current lasting ~ 500 ns. This was noted in both the substrate to body current and between the sample and vacuum chamber implying net charge loss from the body rather than just charge transfer on the object.

4. Solar cells, regardless of size (2x2 or 4x4 cm) or thickness (0.006 or 0.012 in) spontaneously discharged at approximately 9:1 kV (e-gun voltages of 11 to 12 kV). These discharges showed considerable variation in nature and magnitude from less than 1 μ C to much more than 10 μ C.

5. Measurements of charge profiles on solar panel structures demonstrated that the potential above fiberglass around the edges typically exceeds the coverglass potential by approximately 60 percent. A qualitative explanation of the previously observed triggered discharge is that it results from photo-induced charge flow from the fiberglass to the coverslip, followed by a process indistinguishable from spontaneous discharge.

5. Acknowledgements

The authors wish to thank their colleagues W. N. Johnston, Pat Roach, and Norm Hall for mechanical and electrical construction assistance with the experiment execution and data acquisition. We thank Dale Shamblin of FCDNA for his assistance with the data acquisition, and the OWL II crew of the Physics International staff.

6. References

- Bernstein, M.J., "Photoelectron Energy Spectra Generated by Low Energy X-Ray from Intense Plasmas," IEEE Trans. Nucl. Sci., NS-24, 2512 (1977).
- Fromme, D.A., et al., "Electron Emission Spectra Produced by Exploding Wire Photon Sources," IEEE Trans. Nucl. Sci., NS-24, 2429 (1977).
- Fromme, D.A., et al., "SGEMP Response Investigation With Exploding Wire Photons," IEEE Trans. Nucl. Sci., NS-24, 2371 (1977).
- Fromme, D.A., et al., "Exploding Wire Photon Testing of Skynet Satellite," IEEE Trans. Nucl. Sci., NS-25, 1359 (1978).
- Price, M.L., et al., "Electrical and Photon Tests of a Resonant Satellite Shape," IEEE Trans. Nucl. Sci., NS-25, 1358 (1978).
- van Lint, V.A.J., et al., "Spontaneous Discharges and the effects of Electron Charging on Skynet SGEMP Response," IEEE Trans. Nucl. Sci., NS-25, 1293 (1978).
- van Lint, V.A.J., et al., "Skynet Satellite Electron Precharging Experiments," Proceedings of the Spacecraft Charging Technology Conference at the USAFA, November, 1978; NASA Conf. Publication 2071, AFGL-TR-79-0082.

GLOSSARY OF TERMS

EWR	Exploding Wire Radiator. X-ray source which passes very high current through wires for very short times, generating an exploding plasma which gives off low energy photons.
Faraday Cup	Shielded metal cup used to measure charged particle current density in vacuum.
FWHM	Full width at half of the maximum.
Primary electron	Electron liberated by the energy of a photon interacting with an atom.
Secondary electrons	Electrons liberated by interaction with another higher energy electron passing by.
SGEMP	System Generated Electromagnetic Pulse. Electromagnetic waves generated by charges moved by direct photon interaction with systems.
Spacecraft charging	Charging of external spacecraft dielectrics due to natural space radiation.
Spontaneous discharge	Release of stored charge from dielectrics, initiated without any apparent external mechanism.
Teflon, Kapton	Polymer films made by Dupont.
TREK Probe	Instrument made by TREK, Inc. for sensing the potential of a surface without contacting the surface.

DISTRIBUTION LIST

DEPARTMENT OF DEFENSE

Defense Advanced Rsch Proj Agency
ATTN: R. Gullickson

Defense Comm Agency
ATTN: WMMCCS, Sys Engr
ATTN: DWAE-E, B. Hoff

Defense Comm Engr Ctr
ATTN: Code R410, N. Jones
ATTN: Code R401, T. Ellington

Defense Intelligence Agency
ATTN: DB-4C, Rsch, Phys Vuln Br

Defense Nuclear Agency
2 cy ATTN: RAEV
4 cy ATTN: TITL

Defense Tech Info Ctr
12 cy ATTN: DD

Deputy Under Secretary of Defense
Comm, Cmd, Cont & Intell
ATTN: Strat C3 Sys
ATTN: Surveillance & Warning Sys
ATTN: C3IST&CCS
ATTN: Comm Sys

Field Command
Defense Nuclear Agency, Det 1
Lawrence Livermore Lab
ATTN: FC-1

Field Command
Defense Nuclear Agency, Det 2
Los Alamos National Lab/DST
ATTN: MS-635 FC-2

Field Command
Defense Nuclear Agency
ATTN: FCPR
ATTN: FCTT, W. Summa
ATTN: FCTX
ATTN: FCTXE

Interservice Nuclear Weapons School
ATTN: TTV

Joint Chiefs of Staff
ATTN: J-3, Strategic Operations Div
ATTN: GD10, J-5, Nuc & Chem Div
ATTN: C3S Evaluation Office, HDOO

Joint Strat Tgt Planning Staff
ATTN: JLAA
ATTN: JLKS
ATTN: JPSS
ATTN: JLK, DNA Rep
2 cy ATTN: JPTM

National Comm System
ATTN: NCS-TS

DEPARTMENT OF DEFENSE (Continued)

National Security Agency
ATTN: J. Hilton

Program Analysis & Evaluation
ATTN: Strategic Programs

Under Secretary of Defense for Rsch & Engrg
ATTN: AE
ATTN: C3I
ATTN: Strategic & Space Sys (OS)

DEPARTMENT OF THE ARMY

Assistant Chief of Staff for Automation & Comm
ATTN: DAMO-C4

Assistant Secretary of the Army
Rsch, Dev & Acq
ATTN: P. Pierre

BMD Advanced Technology Ctr
ATTN: ATC-0

BMD Systems Cmd
ATTN: BDMSC-H

Deputy Chief of Staff for Rsch, Dev & Acq
ATTN: DAMA-CSS-N

Harry Diamond Labs
ATTN: DELHD-NW-RH, R. Gilbert
ATTN: DELHD-TA-L

US Army Comm Sys Agency
ATTN: CCM-AD-LB, Library

US Army Foreign Science & Tech Ctr
ATTN: DRXST-IS-1

US Army Satellite Comm Agency
ATTN: TACSAT Office
ATTN: Doc Con

USA Missile Cmd
ATTN: Docs Sec.

DEPARTMENT OF THE NAVY

Naval Electronic Systems Cmd
ATTN: PME-106-1

Naval Rsch Lab
ATTN: Code 6707, K. Whitney
ATTN: Code 6611, J. Ritter
ATTN: Code 6701
ATTN: Code 4720, J. Davis

Naval Space Surveillance Sys
ATTN: J. Burton

Naval Surface Weapons Ctr
ATTN: Code F31

DISTRIBUTION LIST

DEPARTMENT OF DEFENSE

Defense Advanced Rsch Proj Agency
ATTN: R. Gullickson

Defense Comm Agency
ATTN: WWMCCS, Sys Engr
ATTN: DWAE-E, B. Hoff

Defense Comm Engr Ctr
ATTN: Code R410, N. Jones
ATTN: Code R401, T. Ellington

Defense Intelligence Agency
ATTN: DB-4C, Rsch, Phys Vuln Br

Defense Nuclear Agency
2 cy ATTN: RAEV
4 cy ATTN: TITL

Defense Tech Info Ctr
12 cy ATTN: DD

Deputy Under Secretary of Defense
Comm, Cmd, Cont & Intell
ATTN: Strat C3 Sys
ATTN: Surveillance & Warning Sys
ATTN: C3IST&CCS
ATTN: Comm Sys

Field Command
Defense Nuclear Agency, Det 1
Lawrence Livermore Lab
ATTN: FC-1

Field Command
Defense Nuclear Agency, Det 2
Los Alamos National Lab/DST
ATTN: MS-635 FC-2

Field Command
Defense Nuclear Agency
ATTN: FCPR
ATTN: FCTT, W. Summa
ATTN: FCTX
ATTN: FCTXE

Interservice Nuclear Weapons School
ATTN: TTV

Joint Chiefs of Staff
ATTN: J-3, Strategic Operations Div
ATTN: GD10, J-5, Nuc & Chem Div
ATTN: C3S Evaluation Office, HDOO

Joint Strat Tgt Planning Staff
ATTN: JLAA
ATTN: JLKS
ATTN: JPSS
ATTN: JLK, DNA Rep
2 cy ATTN: JPTM

National Comm System
ATTN: NCS-1S

DEPARTMENT OF DEFENSE (Continued)

National Security Agency
ATTN: J. Hilton

Program Analysis & Evaluation
ATTN: Strategic Programs

Under Secretary of Defense for Rsch & Engrg
ATTN: AE
ATTN: C3I
ATTN: Strategic & Space Sys (OS)

DEPARTMENT OF THE ARMY

Assistant Chief of Staff for Automation & Comm
ATTN: DAMO-C4

Assistant Secretary of the Army
Rsch, Dev & Acq
ATTN: P. Pierre

BMD Advanced Technology Ctr
ATTN: ATC-0

BMD Systems Cmd
ATTN: BDMSC-H

Deputy Chief of Staff for Rsch, Dev & Acq
ATTN: DAMA-CSS-N

Harry Diamond Labs
ATTN: DELHD-NW-RH, R. Gilbert
ATTN: DELHD-TA-L

US Army Comm Sys Agency
ATTN: CCM-AD-LB, Library

US Army Foreign Science & Tech Ctr
ATTN: DRXST-IS-1

US Army Satellite Comm Agency
ATTN: TACSAT Office
ATTN: Doc Con

USA Missile Cmd
ATTN: Docs Sec.

DEPARTMENT OF THE NAVY

Naval Electronic Systems Cmd
ATTN: PME-106-1

Naval Rsch Lab
ATTN: Code 6707, K. Whitney
ATTN: Code 6611, J. Ritter
ATTN: Code 6701
ATTN: Code 4720, J. Davis

Naval Space Surveillance Sys
ATTN: J. Burton

Naval Surface Weapons Ctr
ATTN: Code F31

DEPARTMENT OF THE NAVY (Continued)

Strategic Systems Project Ofc
ATTN: NSP

DEPARTMENT OF THE AIR FORCE

Air Force Comms Cmd
ATTN: XOT

Air Force Electronic Warfare
ATTN: ESRI 83-0932

Air Force Geophysics Lab
ATTN: PH, C. Pike

Air Force Operational Test & Eval Ctr
ATTN: OAY, Capt Lutz
ATTN: CG

Air Force Soace Technology Ctr
ATTN: A. Gunther

Air Force Tech Applications Ctr
ATTN: TAE

Air Force Weapons Lab
ATTN: SUL
ATTN: NT
ATTN: NTN
2 cy ATTN: NTC

Air University Library
ATTN: AUL-LSE

Assistant Chief of Staff
Studies & Analysis
ATTN: AF/SAMI, Tech Info Div
ATTN: AF/SASC

Ballistic Missile Ofc
ATTN: ENSN
ATTN: ENMG

Deputy Chief of Staff
Rsch, Dev, & Acq
ATTN: AFRDQI
ATTN: AFRDS, Space Sys & C3 Dir

Deputy Chief of Staff
Plans and Operations
ATTN: AFXOS, Opns, Space Div

Office of Space Systems
Office of the Secretary of the Air Force
ATTN: Director

Rome Air Dev Ctr
ATTN: ESR/ET, E. Burke, M/S 64

Headquarters
Space Cmd
ATTN: DC
ATTN: ADCOM DE
ATTN: XPS
ATTN: XPN
ATTN: XPW

DEPARTMENT OF THE AIR FORCE (Continued)

Space Div
ATTN: XR, Plans
ATTN: YDS
ATTN: YEZ
ATTN: YGJ
ATTN: YH, DSCS III
ATTN: YKY
ATTN: YKF
ATTN: YKM
ATTN: YNV

Strategic Air Command
ATTN: XPFS
ATTN: INAS
ATTN: XPQ
ATTN: NRI/STINFO, Library
ATTN: DCZ
ATTN: XPPFR
ATTN: XPFC

OTHER GOVERNMENT AGENCIES

Central Intelligence Agency
ATTN: OSWR/STD/MTB
ATTN: Tech Lib

Department of Commerce
National Oceanic & Atmospheric Admin
ATTN: F. Fehsenfeld

Federal Emergency Management Agency
ATTN: FEMA, Library

NASA
ATTN: Library
ATTN: C. Purvis

DEPARTMENT OF ENERGY CONTRACTORS

University of California
Lawrence Livermore National Lab
ATTN: Tech Info Dept, Library

Los Alamos National Lab
ATTN: Reports Library

Sandia National Labs
ATTN: T. Dellin

Sandia National Labs
ATTN: Org 9336, D. Allen
ATTN: Org 1232, W. Beezhold
ATTN: Tech Library, 3141

DEPARTMENT OF DEFENSE CONTRACTORS

Advanced Rsch & Applications Corp
ATTN: R. Armistead

Aerojet Electro-Systems Co
ATTN: SV/8711/70

Analytic Services, Inc
ATTN: A. Shostak

DEPARTMENT OF DEFENSE CONTRACTORS (Continued)

Aerospace Corp
ATTN: J. Reinheimer
ATTN: V. Josephson, MS-4-933
ATTN: D. Schmunk
ATTN: Library
ATTN: P. Hansen

AVCO Systems Div
ATTN: Library, A830

BDM Corp
ATTN: D. Shaeffer

Beers Associates, Inc
ATTN: B. Beers

Computer Sciences Corp
ATTN: A. Schiff

Dikewood Corp
ATTN: Tech Library

Dikewood Corp
ATTN: K. Lee

EG&G Wash Analytical Svcs Ctr, Inc
ATTN: Library

EOS Technologies, Inc
ATTN: B. Gabbard

General Electric Co
ATTN: J. Peden
ATTN: D. Tasca
ATTN: H. O'Donnell

General Motors Corp
ATTN: MS M-101, T. Nybakken

General Rsch Corp
ATTN: A. Hunt

Hughes Aircraft Co
ATTN: Tech Library

Hughes Aircraft Co
ATTN: A. Narevsky, S32/C332
ATTN: E. Smith, MS V347
ATTN: L. Darda
ATTN: N. Milin, MS B-301

Institute for Defense Analyses
ATTN: Classified Library

IRT Corp
ATTN: N. Rudie
ATTN: B. Williams
ATTN: Library

JAYCOR
ATTN: W. Radasky

JAYCOR
ATTN: Library
ATTN: R. Stahl
ATTN: E. Wenaas

DEPARTMENT OF DEFENSE CONTRACTORS Continued)

JAYCOR
ATTN: R. Sullivan
ATTN: E. Alcaraz

JAYCOR
ATTN: C. Rodgers

JAYCOR
ATTN: R. Poll

JAYCOR
ATTN: M. Bell

Johns Hopkins University
ATTN: P. Partridge

Kaman Sciences Corp
ATTN: Library
ATTN: W. Rich
ATTN: N. Beauchamp
ATTN: D. Osborn

Kaman Sciences Corp
ATTN: E. Conrad

Kaman Tempo
ATTN: DASIAC
ATTN: W. McNamara

Kaman Tempo
ATTN: DASIAC

Lockheed Missiles & Space Co, Inc
ATTN: L. Chase

Lockheed Missiles & Space Co, Inc
ATTN: Dept 85-85

McDonnell Douglas Corp
ATTN: R. Kloster, Dept E451

McDonnell Douglas Corp
ATTN: S. Schneider

Mission Rsch Corp
ATTN: C. Longmire
ATTN: M. Scheibe
ATTN: R. Stettner

Mission Rsch Corp
ATTN: W. Ware

Mission Rsch Corp, San Diego
ATTN: Library
2 cy ATTN: R. Riddell
2 cy ATTN: B. Passenheim
2 cy ATTN: V. van Lint
2 cy ATTN: D. Fromme
5 cy ATTN: Doc Con

Pacific-Sierra Rsch Corp
ATTN: L. Schlessinger
ATTN: H. Brode, Chairman SAGE

R&D Associates
ATTN: Tech Info Ctr
ATTN: S. Siegel

DEPARTMENT OF DEFENSE CONTRACTORS (Continued)

Rand Corp
ATTN: P. Davis

Rand Corp
ATTN: B. Bennett

Rockwell International Corp
ATTN: Library

Rockwell International Corp
ATTN: TIC D/41-092, AJ01

S-CUBED
A Div of Maxwell Labs, Inc
ATTN: A. Wilson
ATTN: Library

DEPARTMENT OF DEFENSE CONTRACTORS(Continued)

Science Applications, Inc
ATTN: W. Chadsey
ATTN: J. Tigner

Science Applications, Inc
ATTN: K. Sites

SRI International
ATTN: Library

SRI International
ATTN: A. Padgett

TRW Electronics & Defense Sector
ATTN: Tech Info Ctr
ATTN: D. Clement
ATTN: R. Kingsland

DATE
FILME